

Study of cross-shell excitations near the 'island of inversion' using fusion-evaporation and Doppler shift methods

Jonathan Williams (TRIUMF)

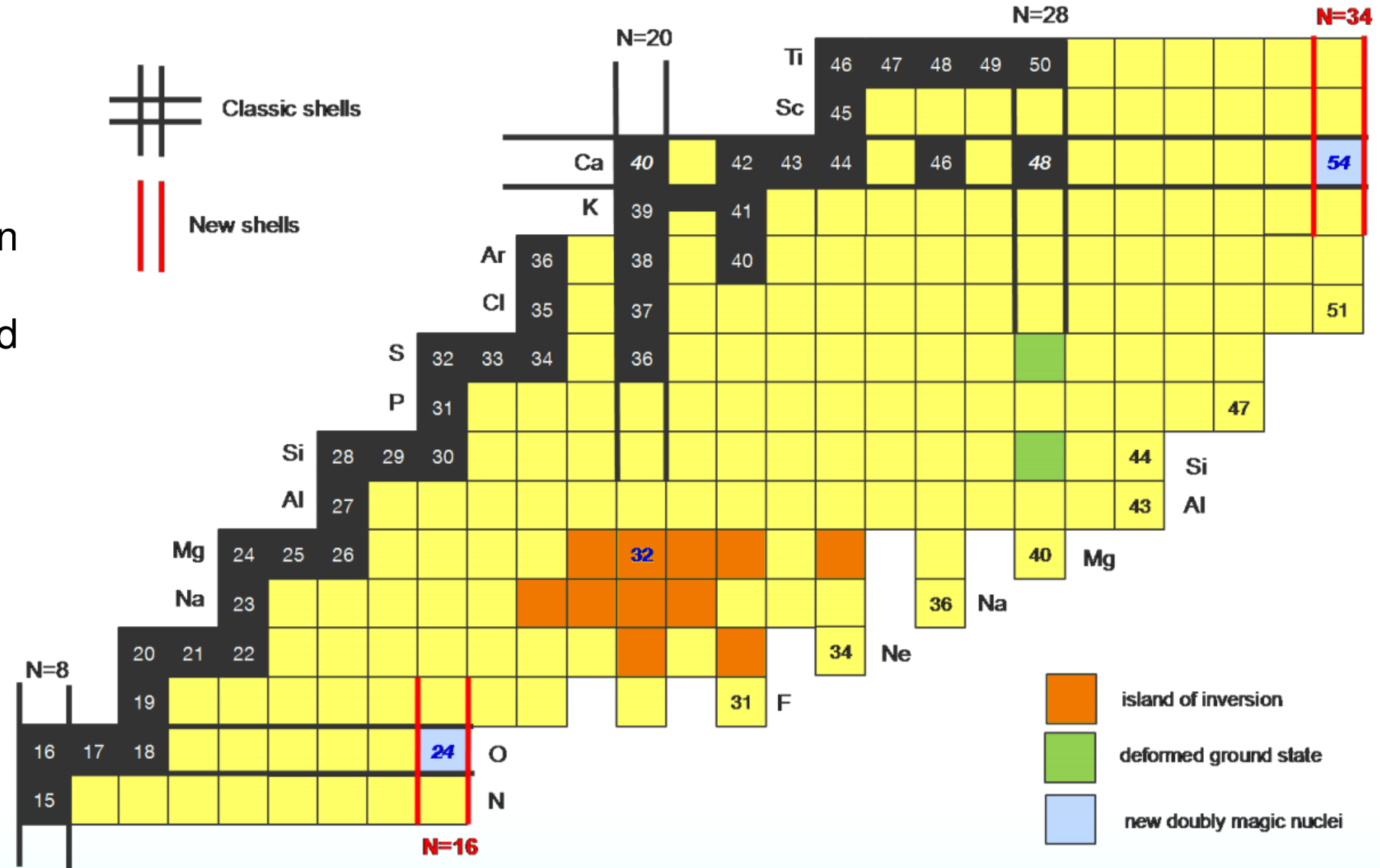
For TIP and TIGRESS

Nuclear Structure 2022 – June 16

Berkeley, California

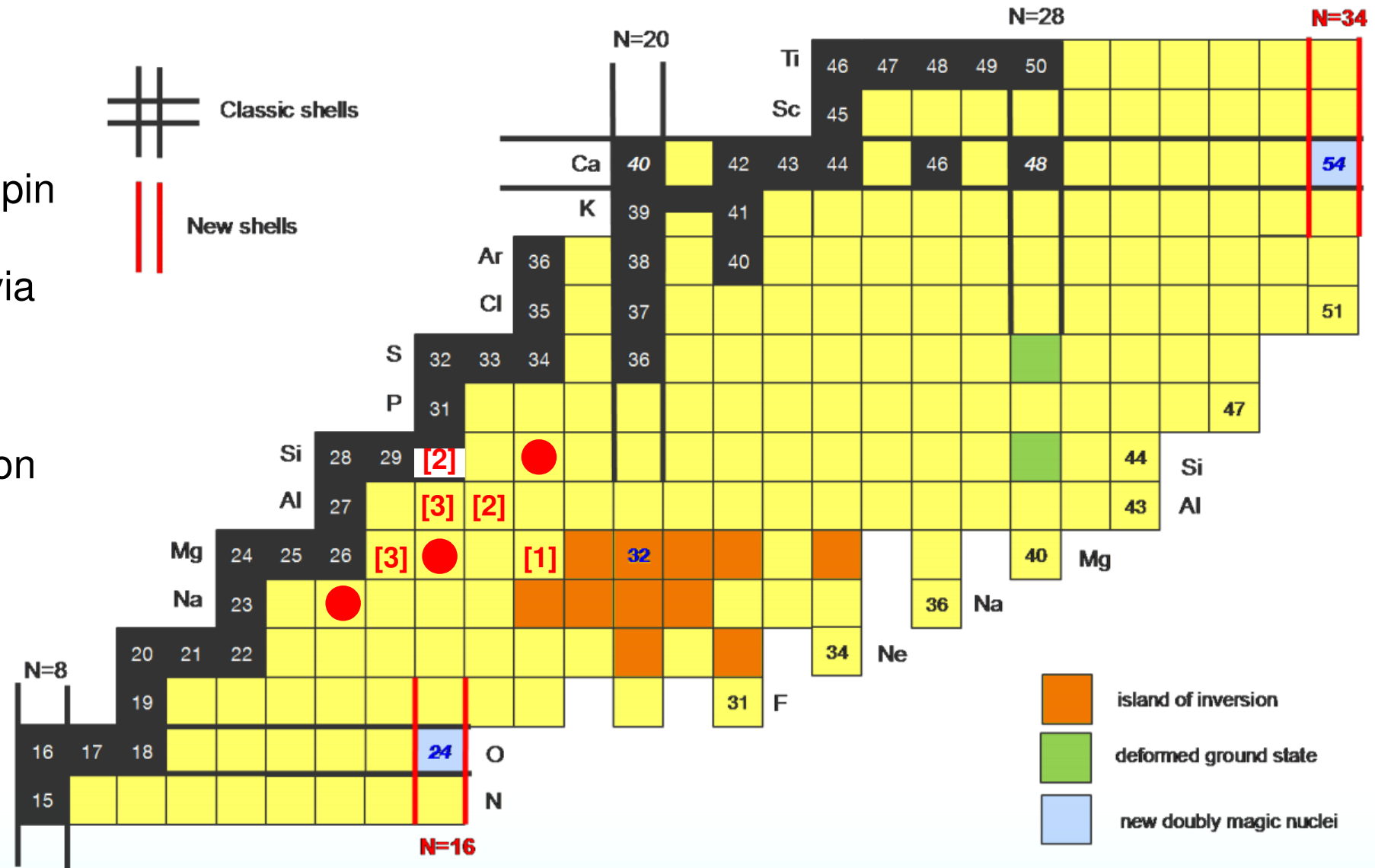
Background

- At the N=20 'island of inversion' around ^{32}Mg , residual nucleon-nucleon interactions and shell evolution result in ground states with neutrons in the *pf* shell.
- For less neutron-rich species in the *sd* shell, similar configurations occur at high energy.
- Data on these 'cross-shell' excited states gives insight into shell evolution, but is limited for many nuclides.



Background

- Recent studies have investigated the higher-spin regime (likely to contain cross-shell excitations) via fusion-evaporation reactions.
- Needs channel separation via particle or recoil identification, and/or γ coincidence gating.
- Lifetime information is also useful for identifying intruder states.



Some recent studies of high-spin states:

[1] A. N. Deacon et al., *PRC* 82 034305 (2010).

[2] D. Steppenbeck et al., *Nucl Phys A* 847 149-167 (2010).

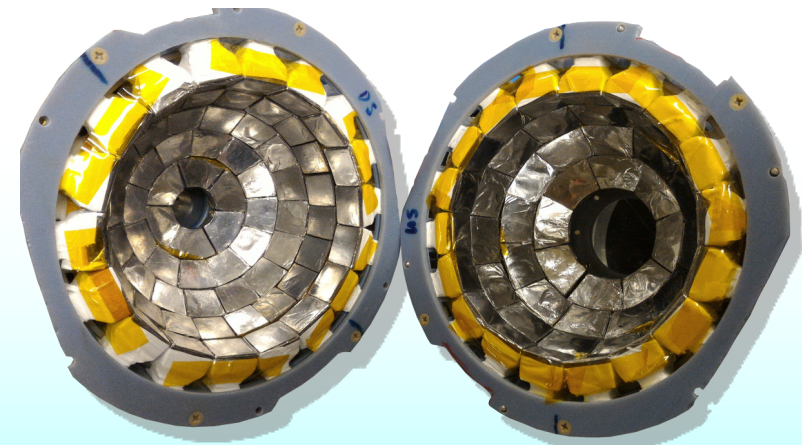
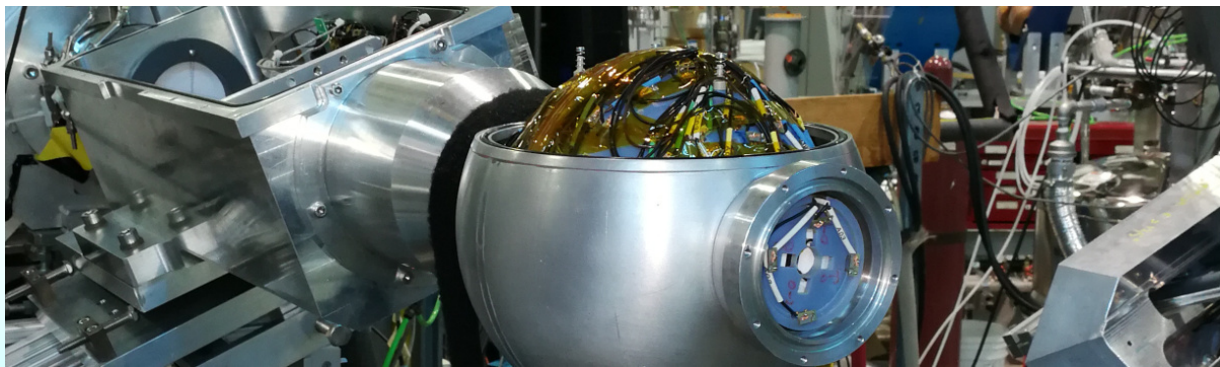
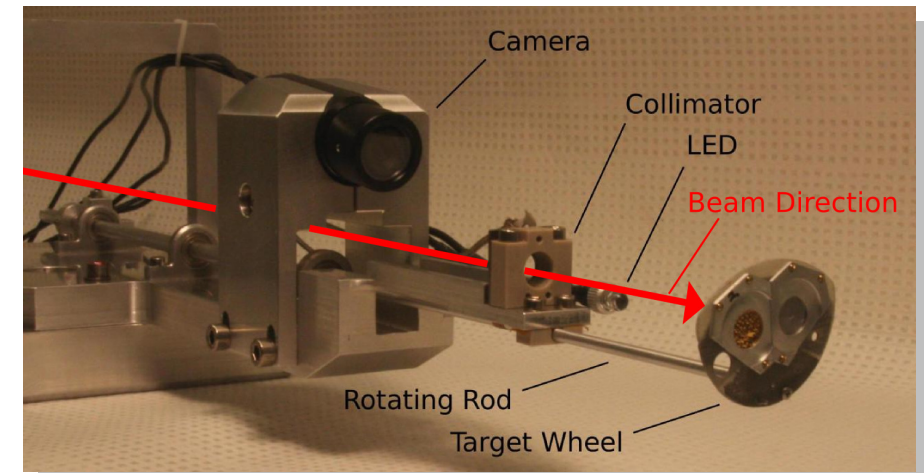
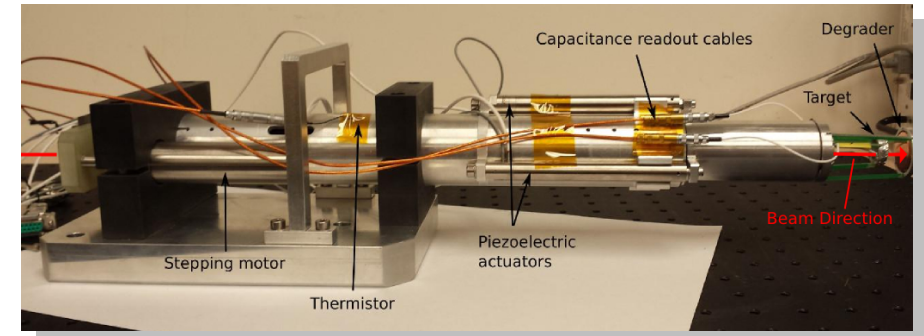
[3] R. Dungan et al., *PRC* 94 064305 (2016).

● Nuclides covered in this talk

TIP Overview

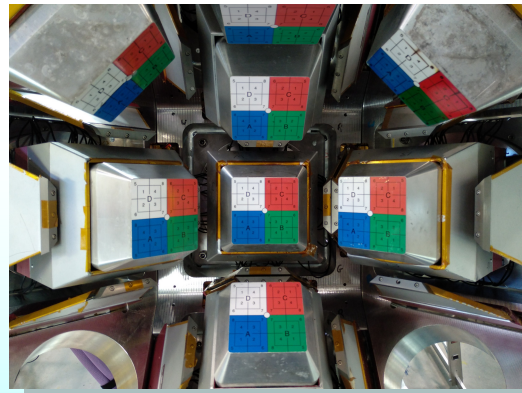
Program developed at Simon Fraser University, focused on lifetime measurements using Doppler shift methods.

- Lifetimes > 1 ps measured via the Recoil Distance Method (RDM) using a plunger device.
- Lifetimes < 1 ps measured via the Doppler Shift Attenuation Method (DSAM) using a backed target.
- CsI(Tl) “ball” array for charged particle detection/identification.
- Target chamber which can be integrated with TIGRESS (γ -ray spectrometer) and/or EMMA (recoil separator).

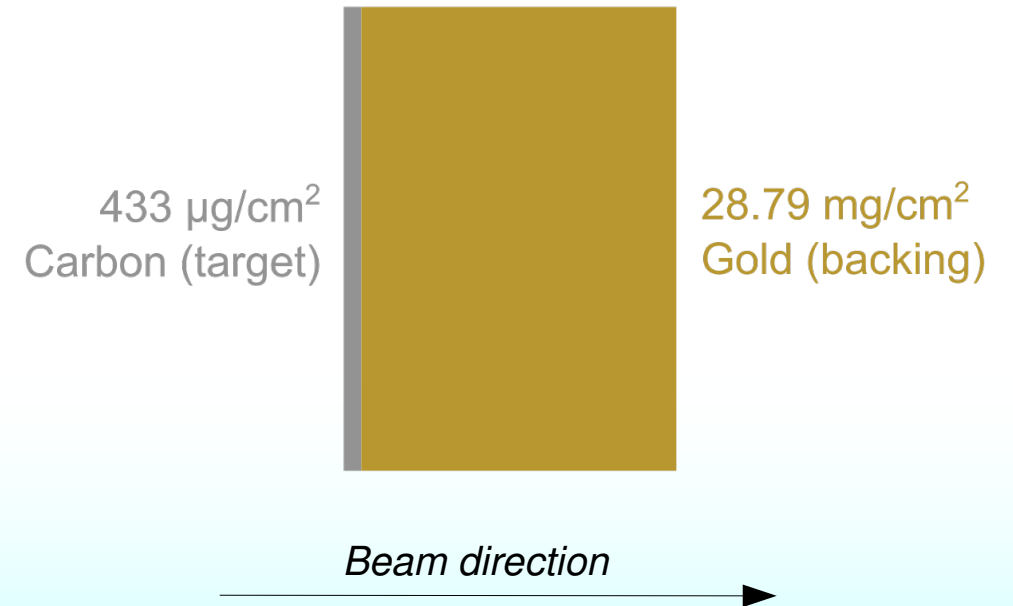
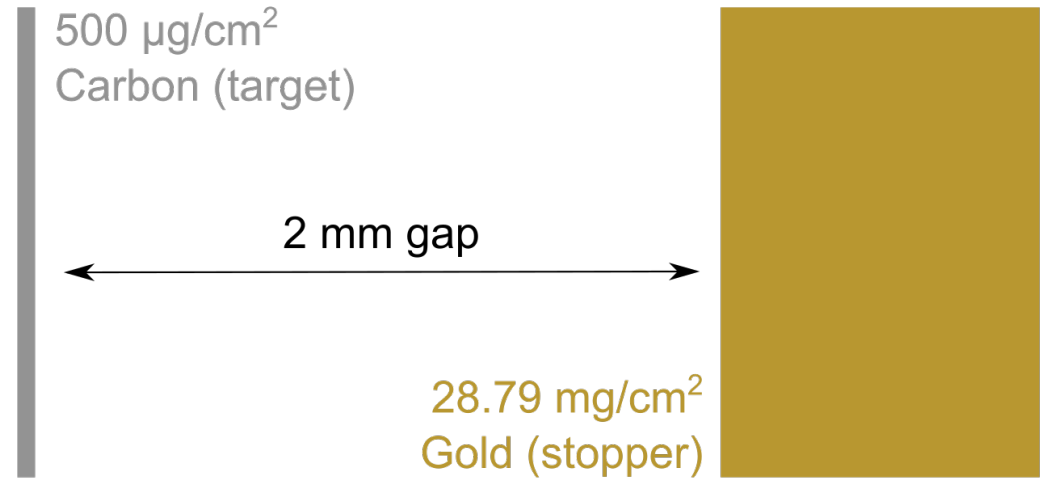


Configuration for this experiment

- ^{18}O beam @ $\sim 10^{10}$ pps, 48 MeV, $^{\text{nat.}}\text{C}$ targets.
 - Channels of interest: ^{25}Na (αp), ^{28}Mg ($2p$)
- Run time split between a thin target (~ 21 hours) for coincidence spectroscopy and a DSAM target (~ 40.5 hours) for lifetime measurements.
- 38-element partial CsI ball.
- 13 TIGRESS clovers in 4/5/4 configuration.

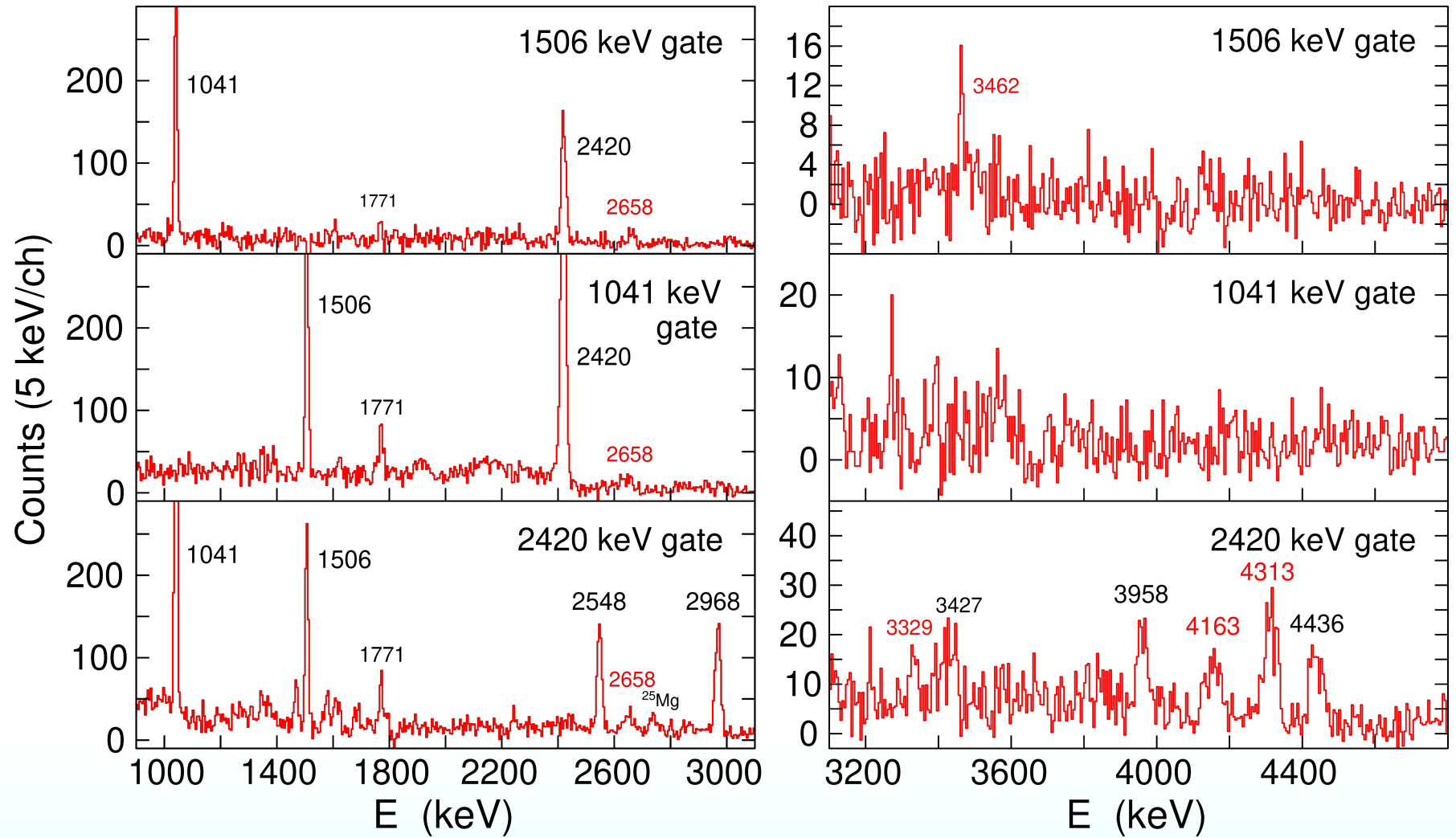


(Not to scale)



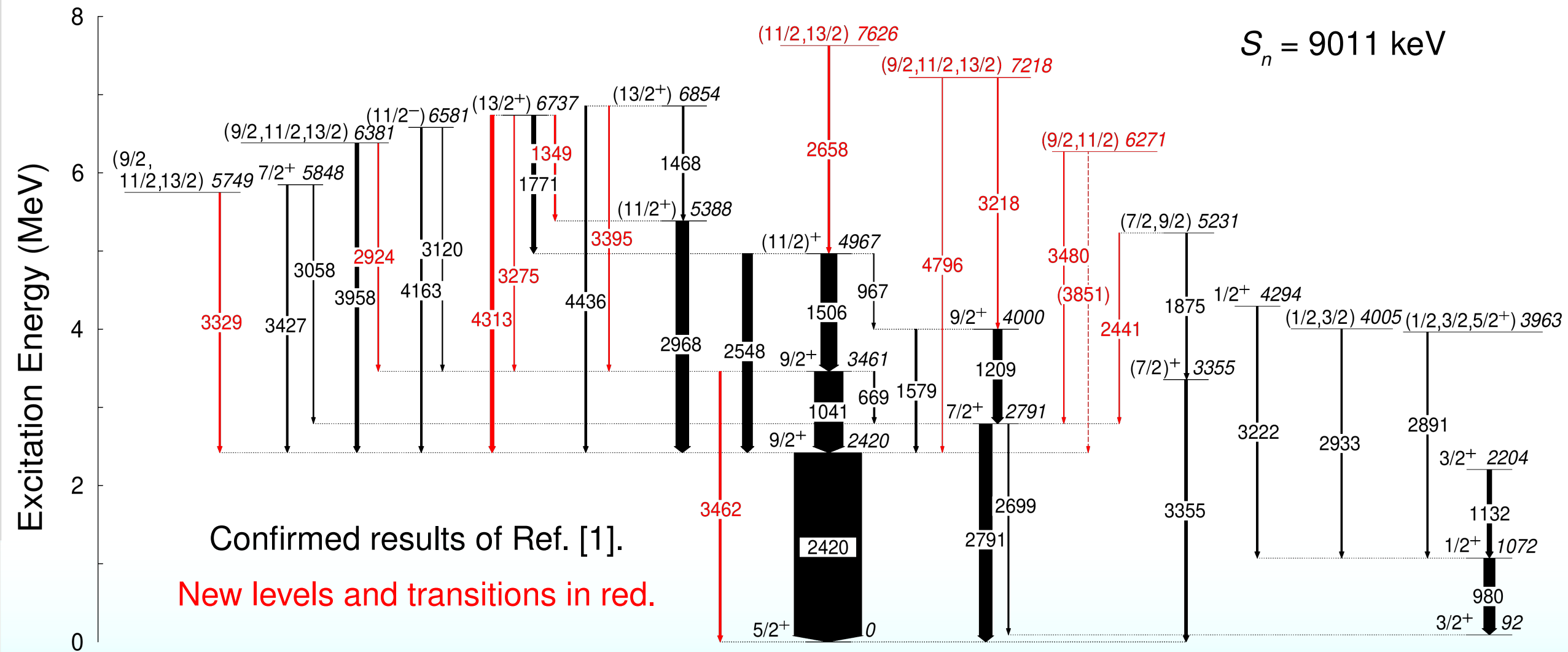
^{25}Na thin target results

- ^{25}Na was populated using the $^{12}\text{C}(^{18}\text{O},\alpha p)$ reaction.
- Strong population of a “main band” of 2420, 1041, and 1506 keV transitions.
- Some previously unobserved transitions (labels in red) at high energies.



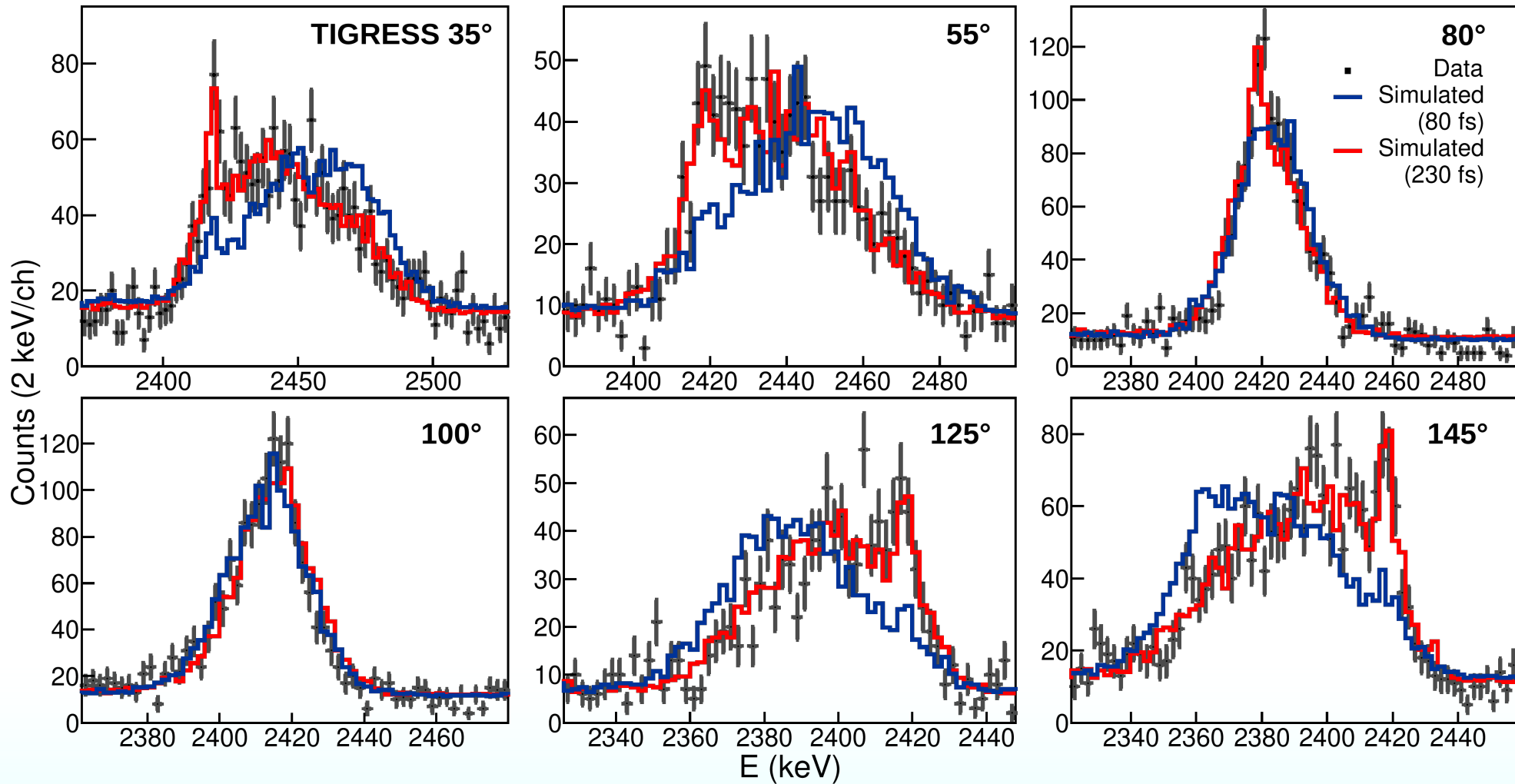
^{25}Na γ -gated spectra (thin target, Doppler corrected).

^{25}Na full level scheme



[1] J. M. VonMoss et al., PRC 92 034301 (2015)

^{25}Na DSAM results

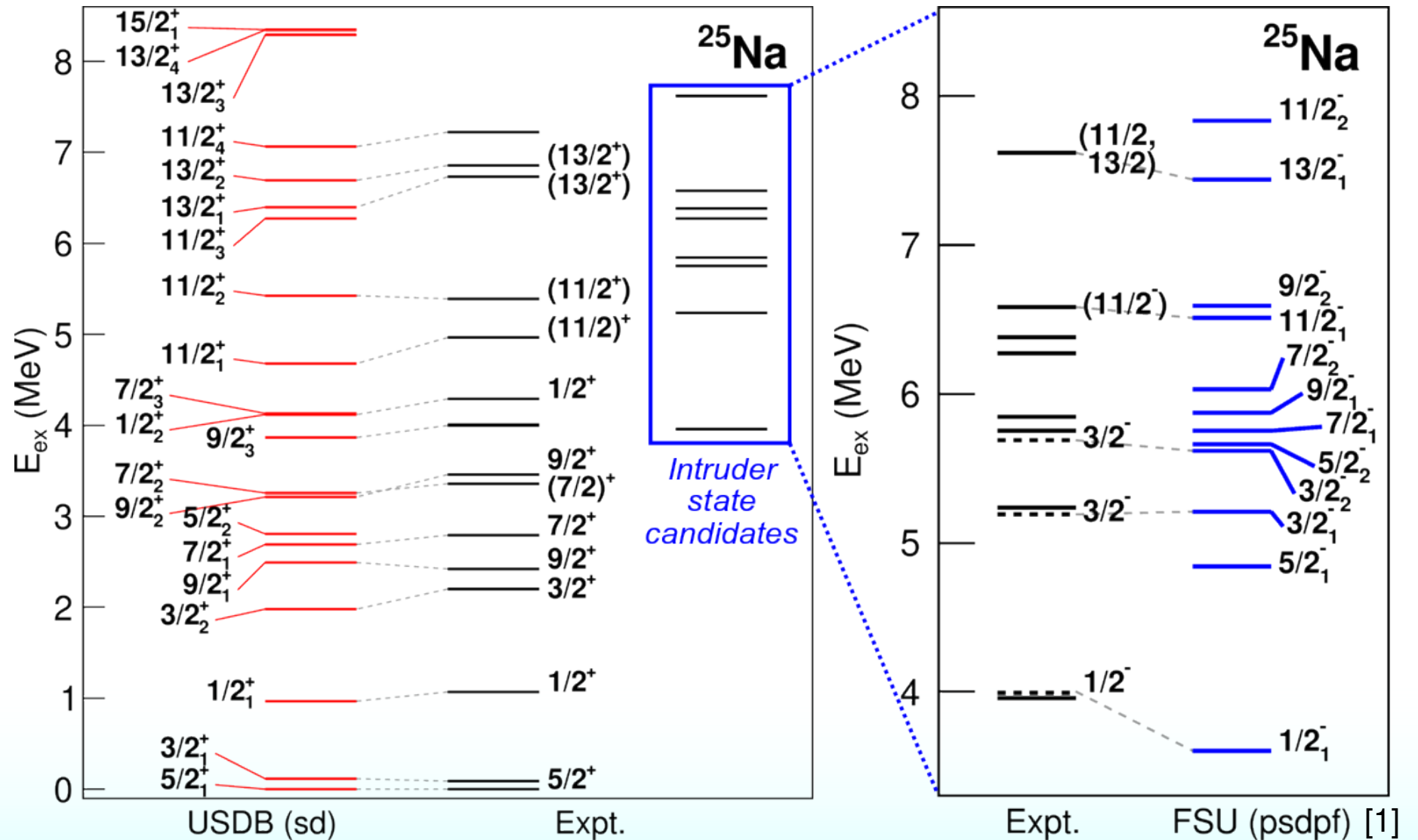


- Comparison to GEANT4 simulations, using maximum-likelihood χ^2 method.
- Feeding corrected by gating from above and simulating the effect of the feeding transition.

^{25}Na 2420 keV transition, simulation @ $\tau_{\text{mean}} = 230(40)$ fs

^{25}Na calculations (sd shell)

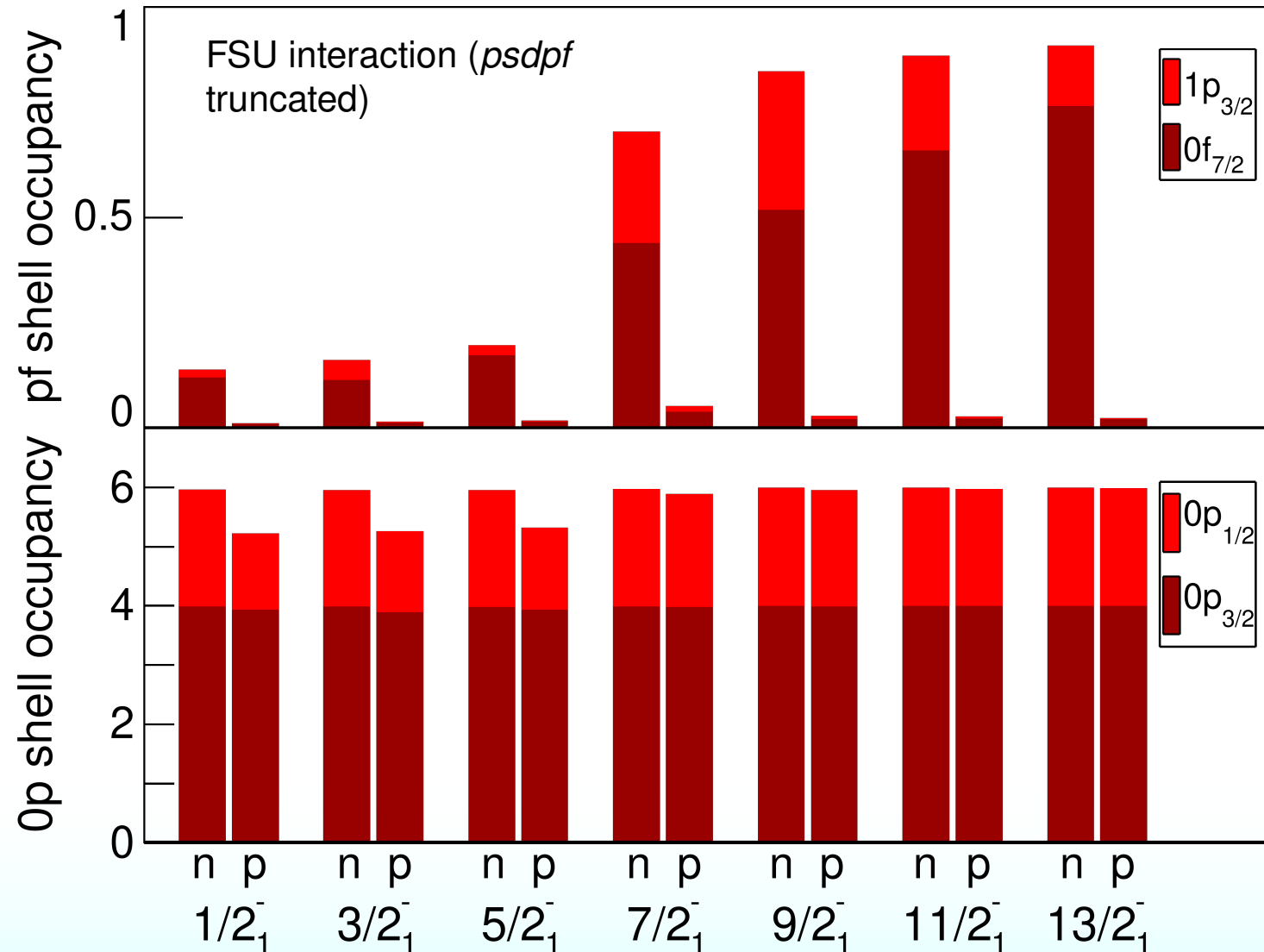
- Low-lying states are well reproduced in USDB calculations in the *sd* shell.
- Some high-lying states don't fit in well and are intruder state candidates.
- Highest energy state @ 7626(4) keV most likely negative parity.



^{25}Na calculations (cross-shell occupancies)

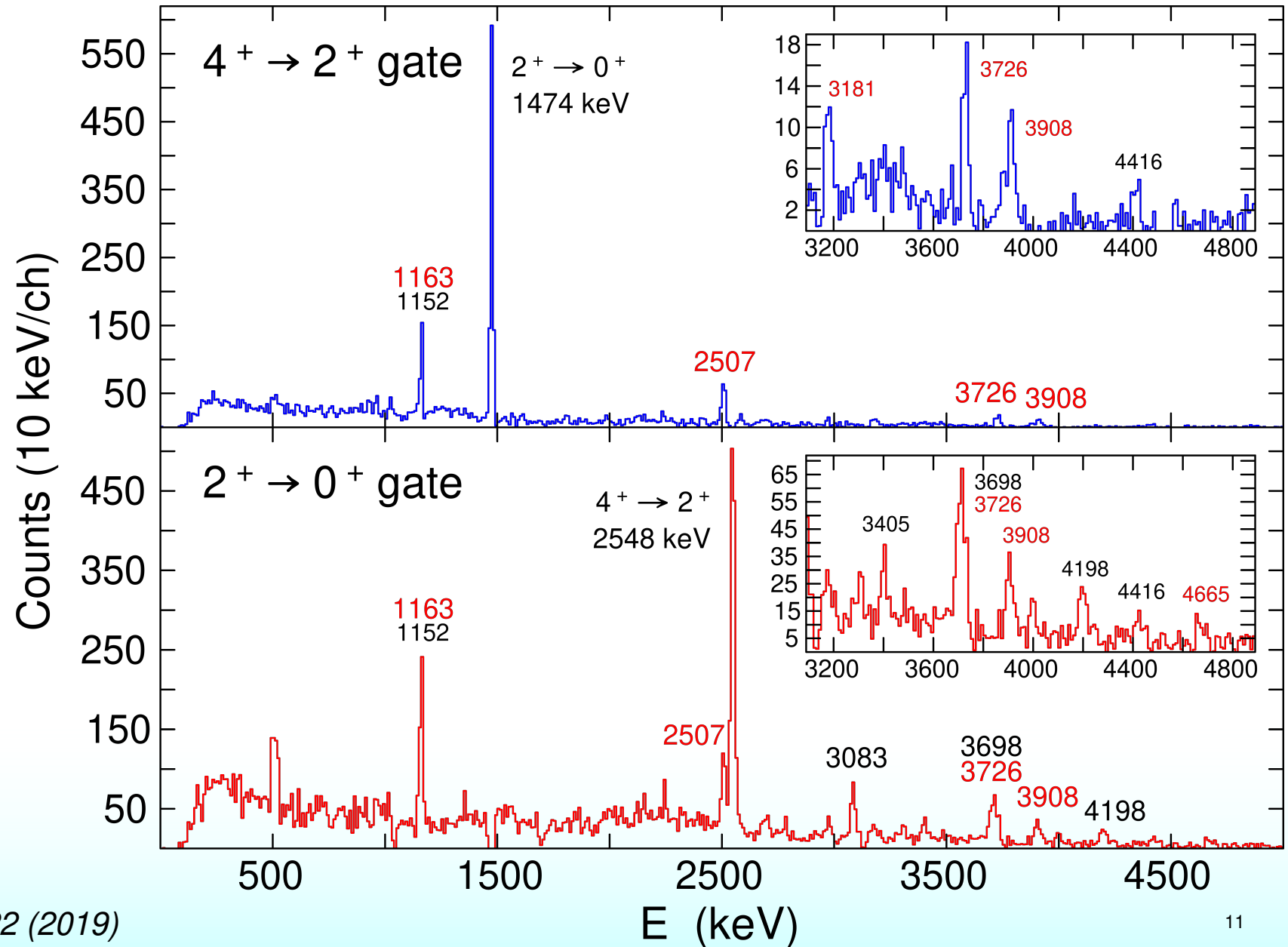
Calculated pf orbital occupancies of $1p1h$ intruder states in ^{25}Na show differing excitation modes:

- Low spin: proton excitation from the $0p$ shell.
- High spin: neutron excitation to the upper pf shell.

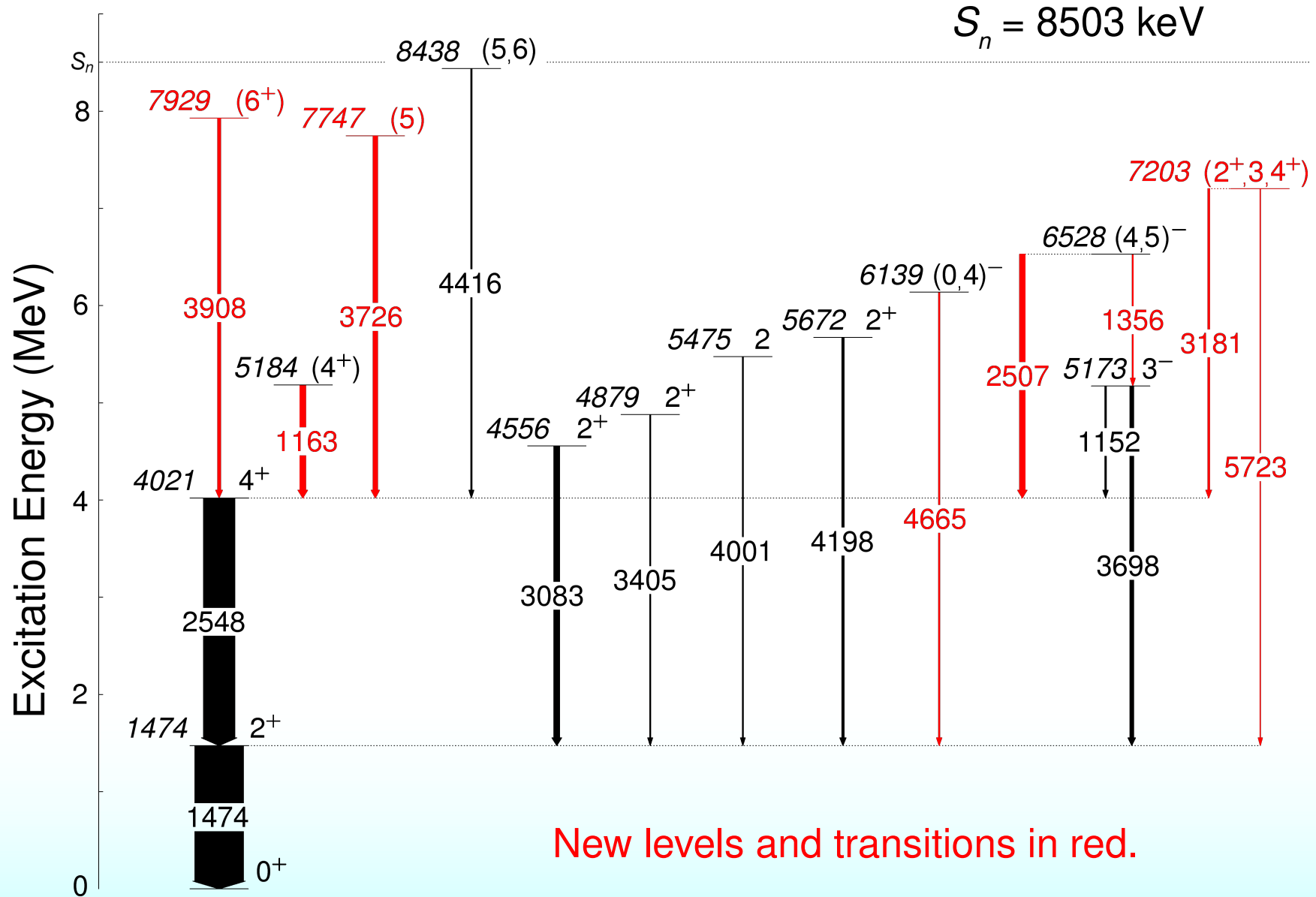


^{28}Mg thin target results

- ^{28}Mg was populated using the $^{12}\text{C}(^{18}\text{O},2p)$ reaction.
- A large fraction of transitions are newly observed (labels in red), including some of the most intense.

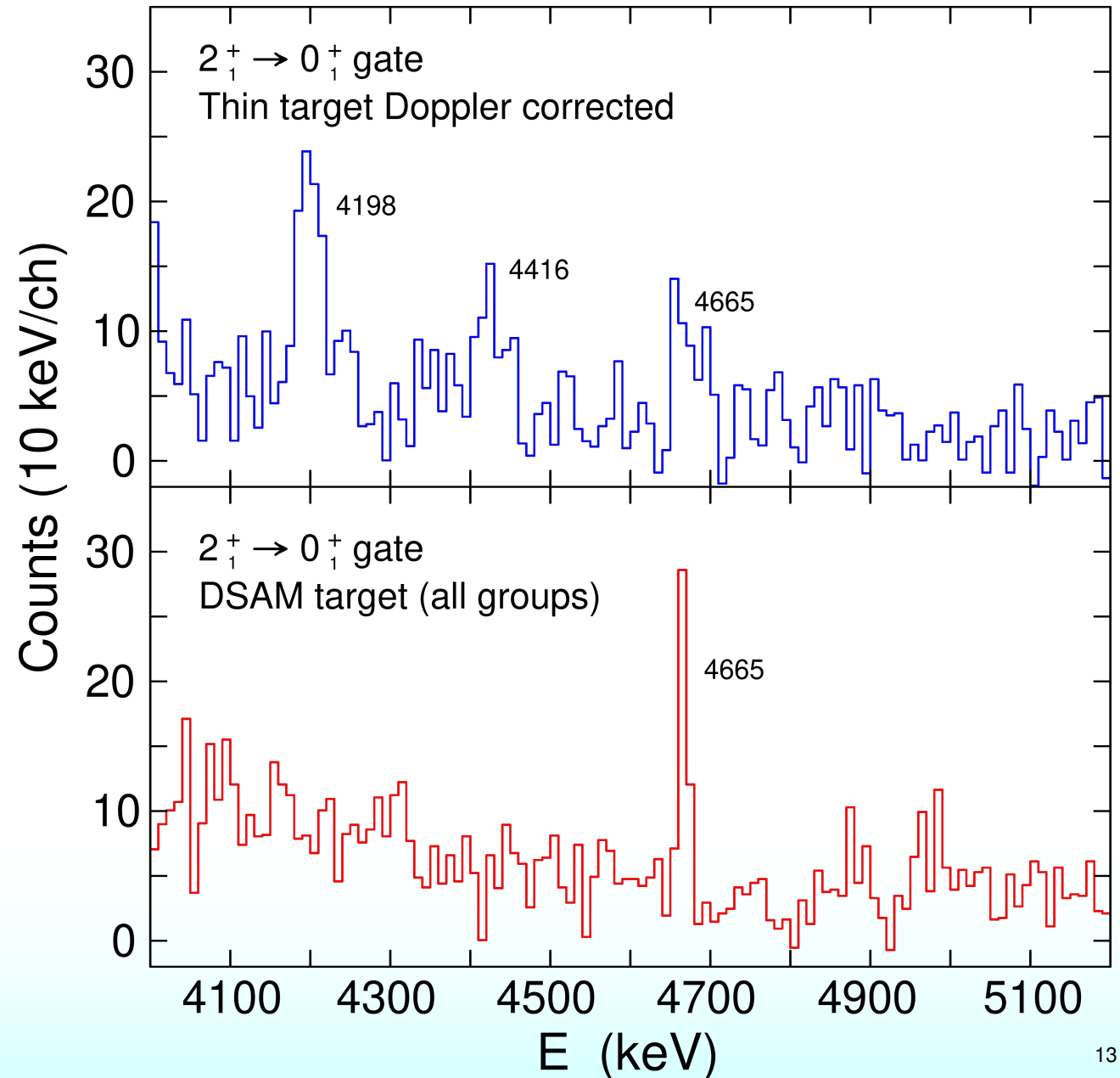


^{28}Mg level scheme



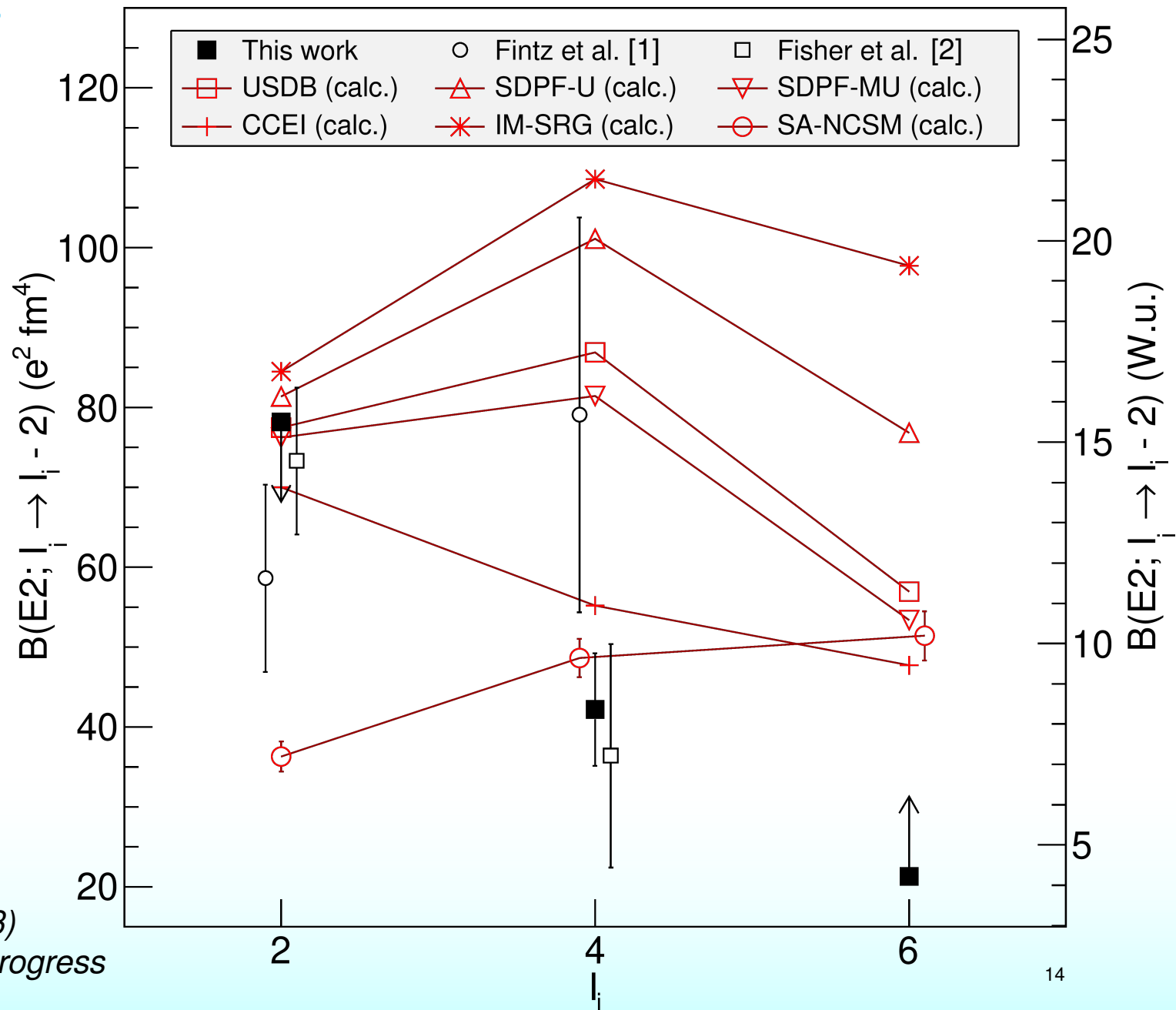
^{28}Mg long-lived level

- Long lived level at 6139 keV:
 - 4664.9(12) keV transition stopped in DSAM target data.
 - Doppler shifted in thin target data.
- Inferred level lifetime: > 1 ps, < 250 ps.
- Suggests transition of M2 or higher multipolarity, level $I^\pi = 0^-$ or 4^-
- Similar isomer in nearby ^{32}Si , also negative parity.



^{28}Mg yrast band $B(E2)$ values

- $B(E2)$ values along yrast band trend lower than most model calculations.
- Ab-initio SA-NCSM [3] calculations agree well with $B(E2; 4^+ \rightarrow 2^+)$ from this data, but disagree with previous data.
 - Plunger data taken to measure $B(E2; 2^+ \rightarrow 0^+)$ populated using the same reaction (M. S. Martin, SFU).



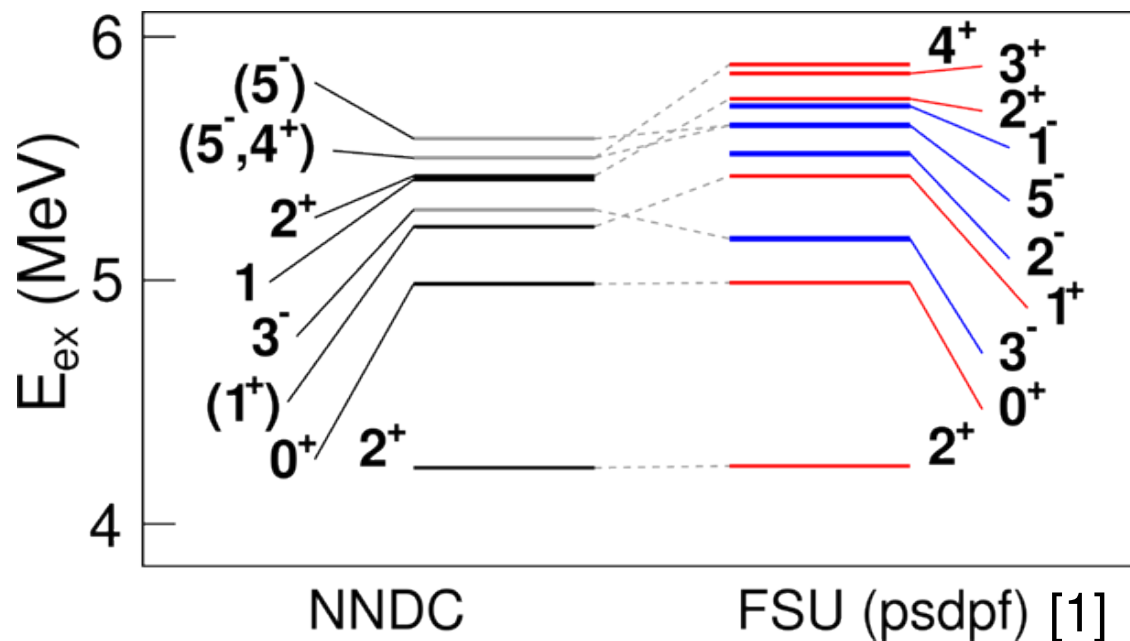
[1] P. Fintz et al., *Nucl. Phys. A* 197, 423 (1972)

[2] T. R. Fisher et al., *Phys. Rev. C* 7, 1878 (1973)

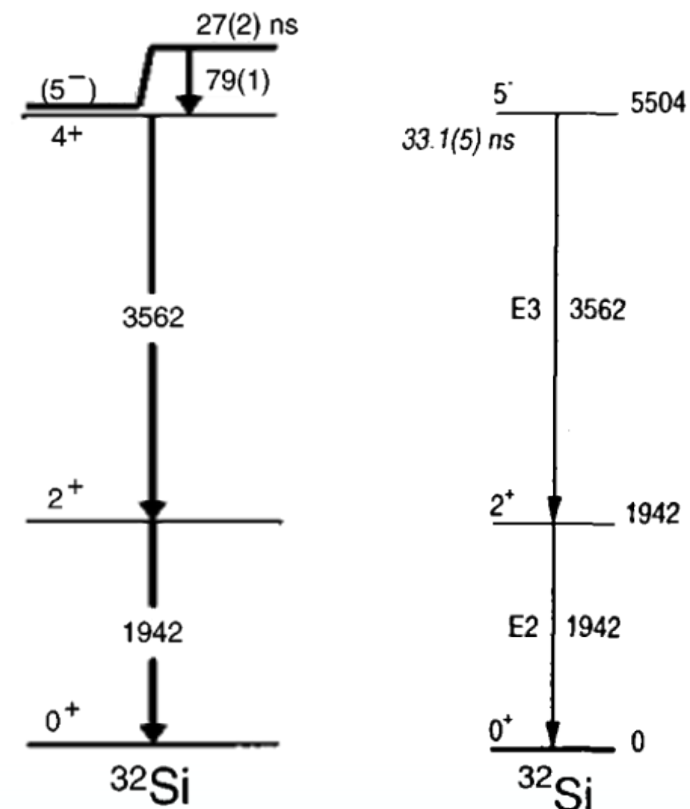
[3] K. D. Launey, T. Dytrych, and J. P. Draayer, *Progress in Particle and Nuclear Physics* 89, 101 (2016)

Future plans - ^{32}Si

Cross-shell excitations in ^{32}Si will be investigated with the $^{22}\text{Ne}(^{12}\text{C},2p)$ reaction. Goals are to obtain improved lifetime measurements, measure angular distributions, and determine the placement of the $I^\pi = (5^-)$ nanosecond isomer.



Calculated levels at intermediate energies in ^{32}Si .



Fornal et al. [2]

Asai et al. [3]

Proposed decay schemes of the nanosecond isomer.

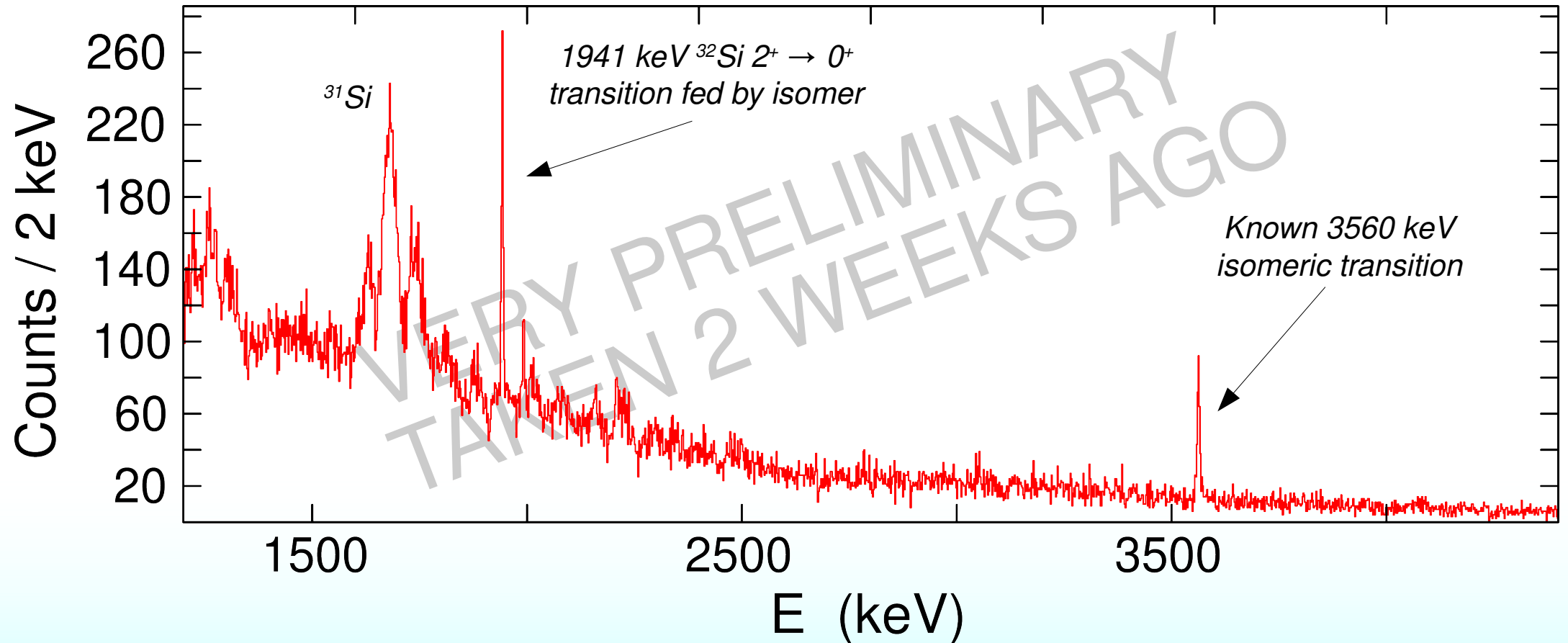
[1] R. S. Lubna, et al., *Phys. Rev. Research* 2 043342 (2020)

[2] B. Fornal et al., *Phys. Rev. C* 55 762 (1997)

[3] M. Asai et al., *JAERI Tandem Annual Report 2001*, 23 (2002)

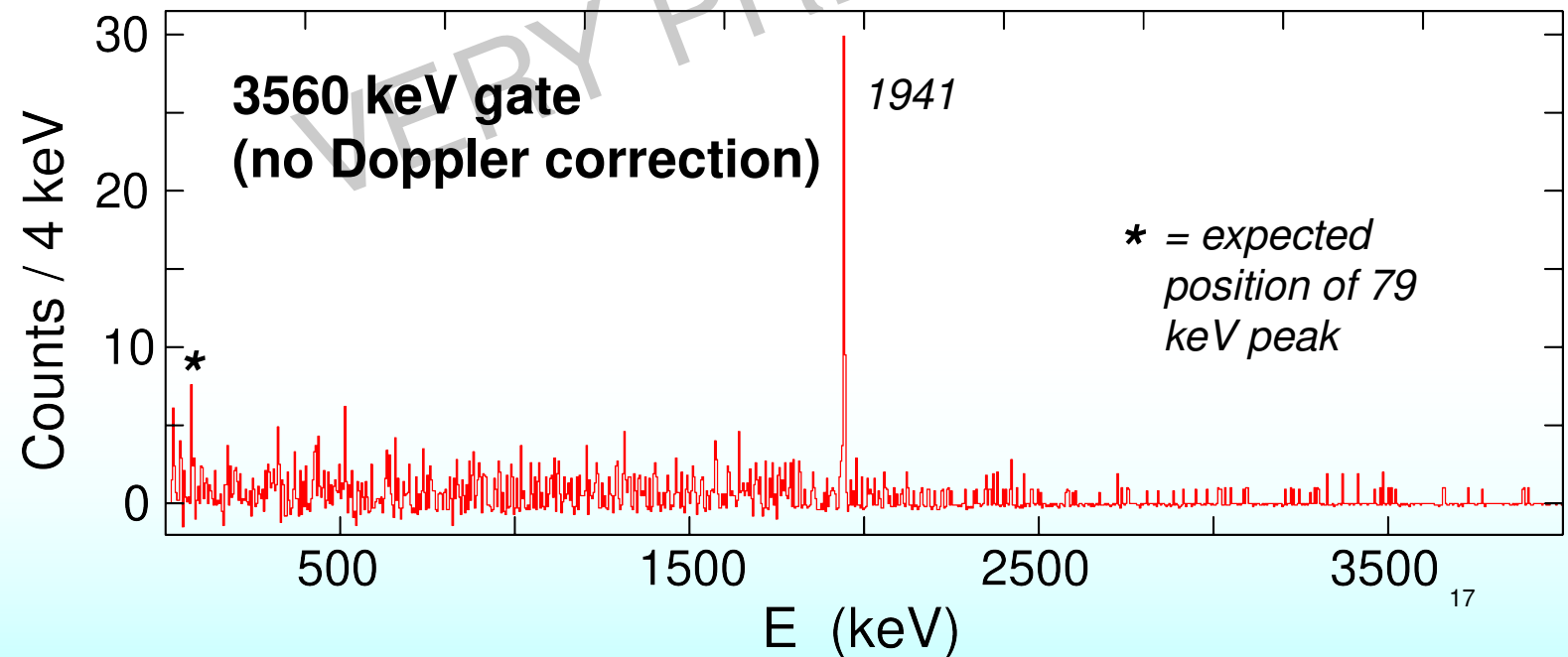
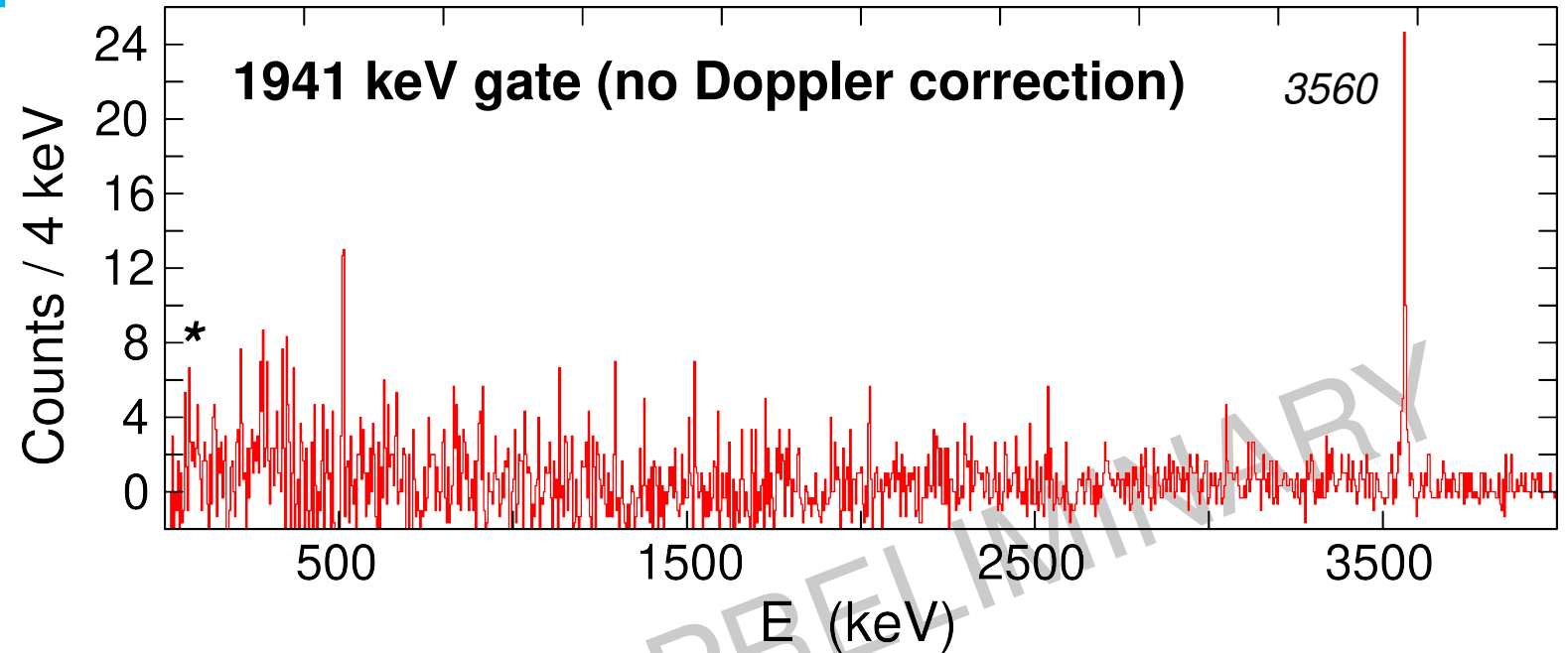
^{32}Si test data – singles

Initial test data taken with a ^{12}C thin target + downstream ^{197}Au stopper shows population of the isomer. Analysis of this data will inform plans to run the full experiment in the coming year.



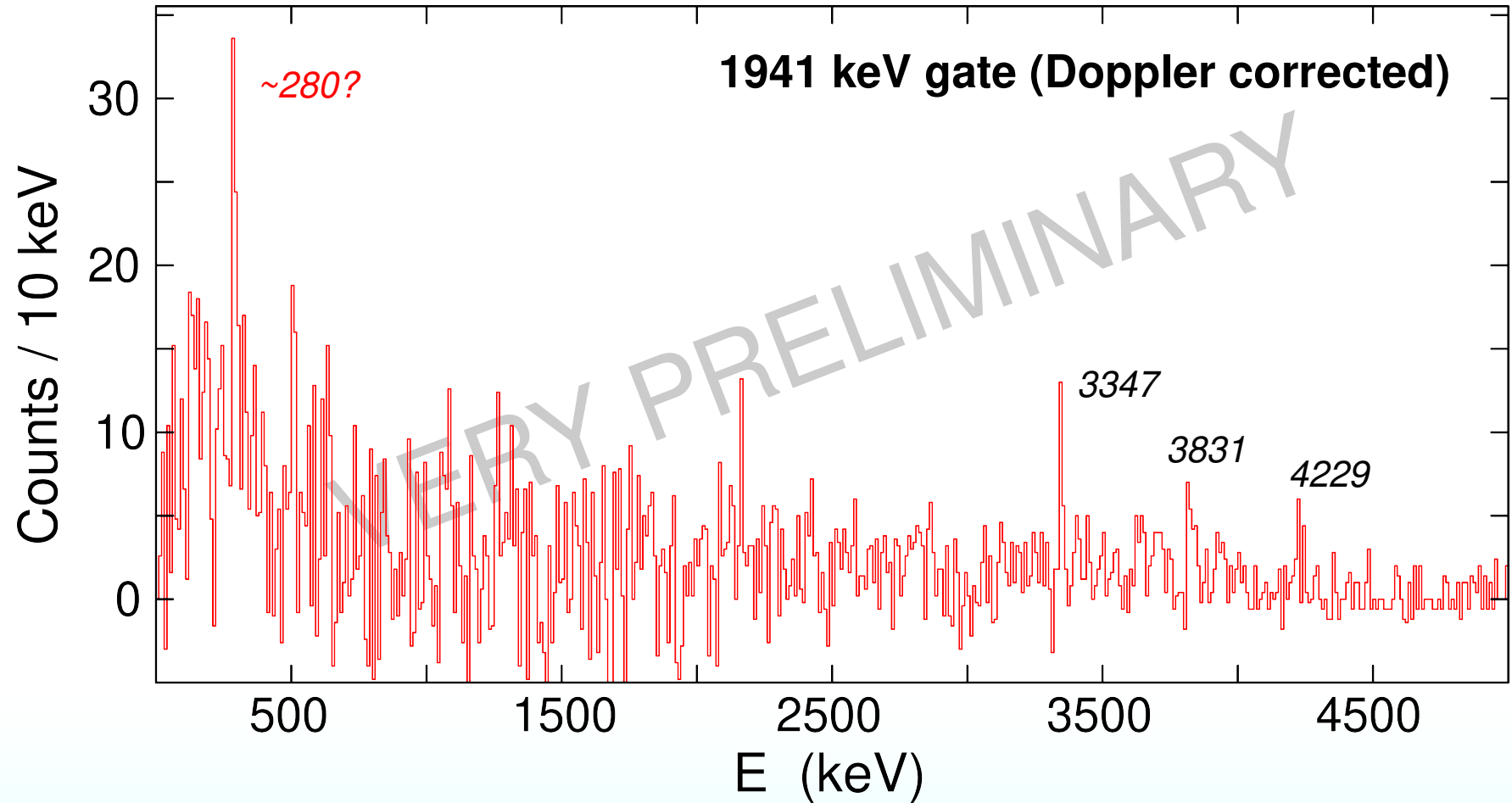
^{32}Si test data – the isomer

- No evidence yet of the 79 keV isomeric transition assumed in NNDC (expect $>1/2$ the counts of the 1941 keV line).
 - Suggests a $5^- \rightarrow 2^+_1$ E3 transition.
 - $B(E3)\downarrow$ would be $\sim 100\times$ lower than values in nearby ^{36}Cl and ^{39}K .
- If true, then the 4^+_1 state in ^{32}Si is not yet assigned (maybe we can do it).



^{32}Si test data – prompt transitions

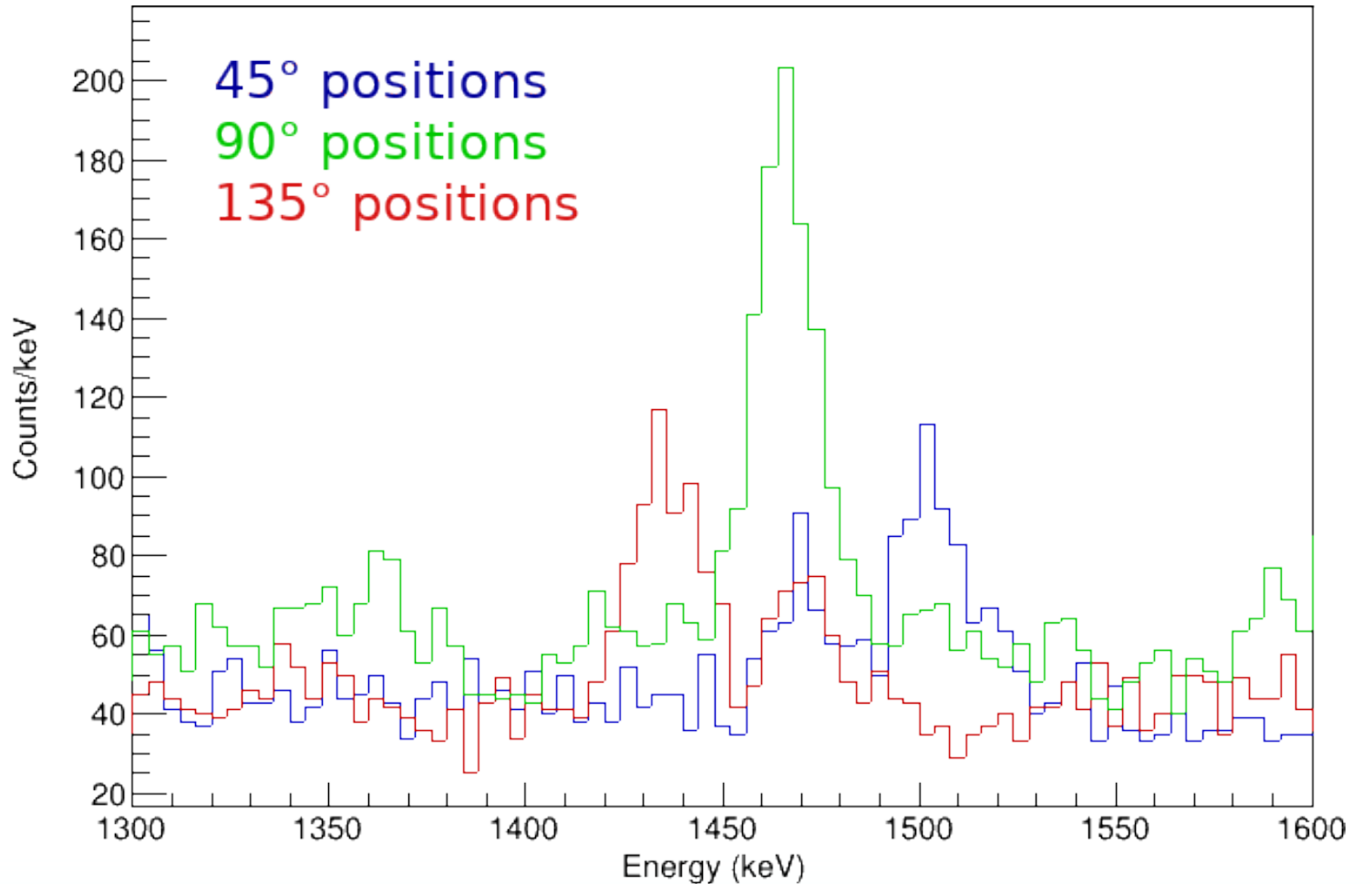
- Doppler corrected data shows that the 2^+_{1} level is also populated by prompt transitions.
 - Includes known $3^-_{1} \rightarrow 2^+_{1}$ transition.
 - No immediately obvious indication of a 4^+_{1} level.
- More data coming soon™.



Recent TIP experiments: ^{28}Mg RDM

Follow-up to the earlier DSAM measurements in ^{28}Mg .

- Aims to measure $B(E2; 2^+_{1} \rightarrow 0^+_{1})$ and investigate the discrepancy with ab-initio SA-NCSM calculations.
- May also measure the lifetime of the long-lived state at 6139 keV.
- Beamtime in 2021, data under early analysis.



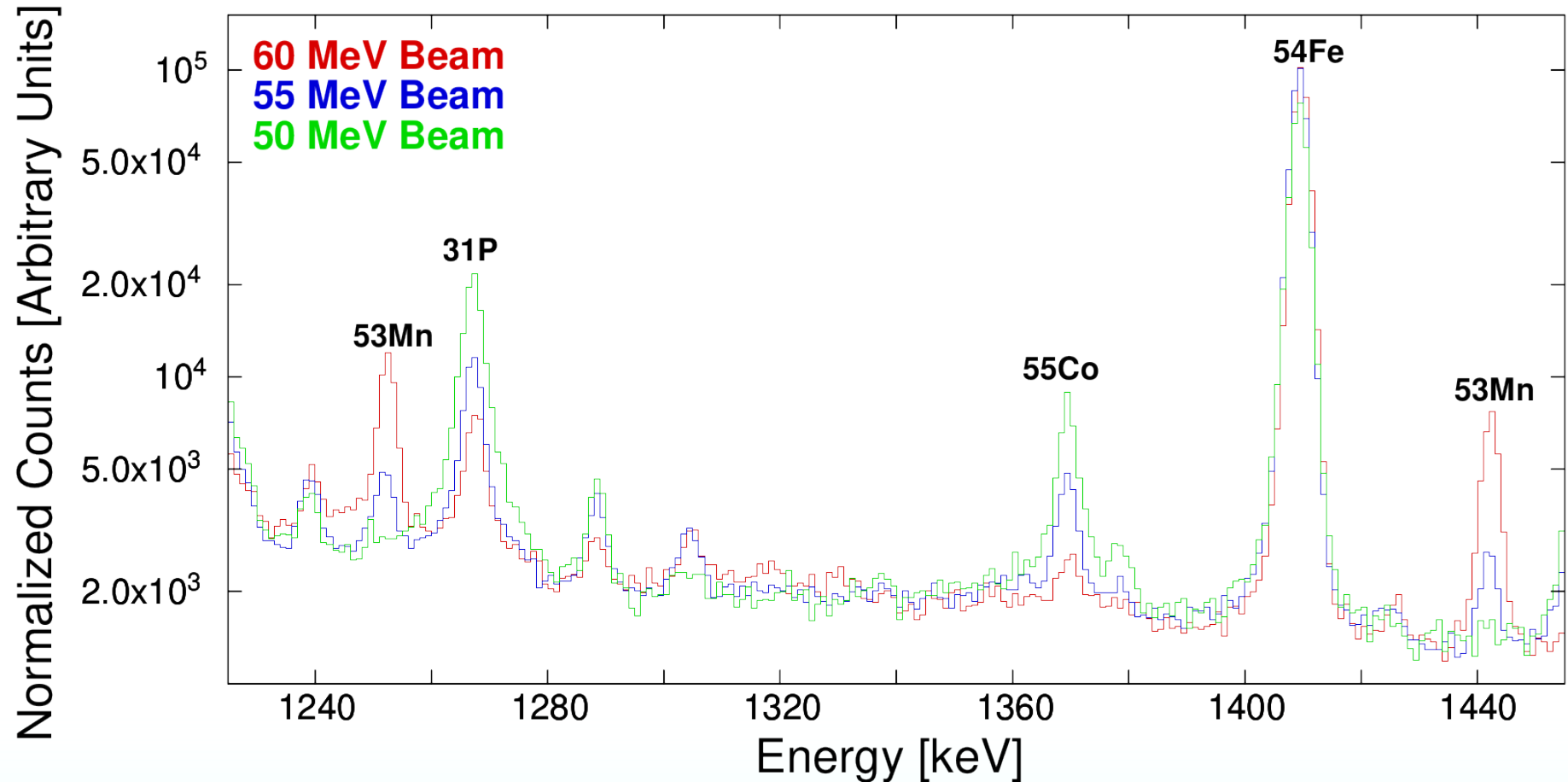
Plunger spectra of the $2^+_{1} \rightarrow 0^+_{1}$ transition in ^{28}Mg (51.5 μm separation).

Poster: Electromagnetic Transition Rate Studies in ^{28}Mg (M. S. Martin, SFU)

Recent TIP experiments: $A=55$ mirror symmetry

Study of mirror symmetry in $A=55$ nuclei (^{55}Co , ^{55}Ni) populated using fusion-evaporation.

- ^{55}Co via stable beam: $^{40}\text{Ca}(^{20}\text{Ne}, \alpha p)^{55}\text{Co}$.
- ^{55}Ni via radioactive beam: $^{40}\text{Ca}(^{20}\text{Na}, \alpha p)^{55}\text{Ni}$.
- Stable beam portion completed June 2022.



Poster: Mirror Symmetry in the $f_{7/2}$ Shell Below ^{56}Ni , Excited States and Electromagnetic Transition Rates in ^{55}Ni and ^{55}Co (H. Asch, SFU)

Summary

Experimental results:

- Extension of level schemes in ^{25}Na and ^{28}Mg in the high energy/spin regime.
 - Higher energy states in ^{25}Na not well reproduced by USDB, are probable intruder states.
 - Long-lived intruder state in ^{28}Mg .
- Also studied ^{22}Ne (2α channel) and found several new transitions/levels.
- Initial ^{32}Si data shows nanosecond isomer population.

Ongoing and future work:

- Analysis of plunger data on ^{28}Mg (M. S. Martin, SFU).
- Study of $A=55$ mirror nuclei ($^{55}\text{Co}/^{55}\text{Ni}$) using fusion-evaporation with a radioactive ^{20}Na beam (H. Asch, SFU).
- Follow up study of cross-shell excitations in ^{32}Si .

Acknowledgments

Simon Fraser University – H. Asch, A. Chester, T. Domingo, M. S. Martin, P. Spagnoletti, K. Starosta, K. Whitmore

TRIUMF - G. C. Ball, A. B. Garnsworthy, G. Hackman, J. Henderson, R. Henderson, V. Karayonchev, R. Krücken, R. S. Lubna, J. Measures, O. Paetkau, J. Park, D. Rhodes, J. Smallcombe, M. Williams

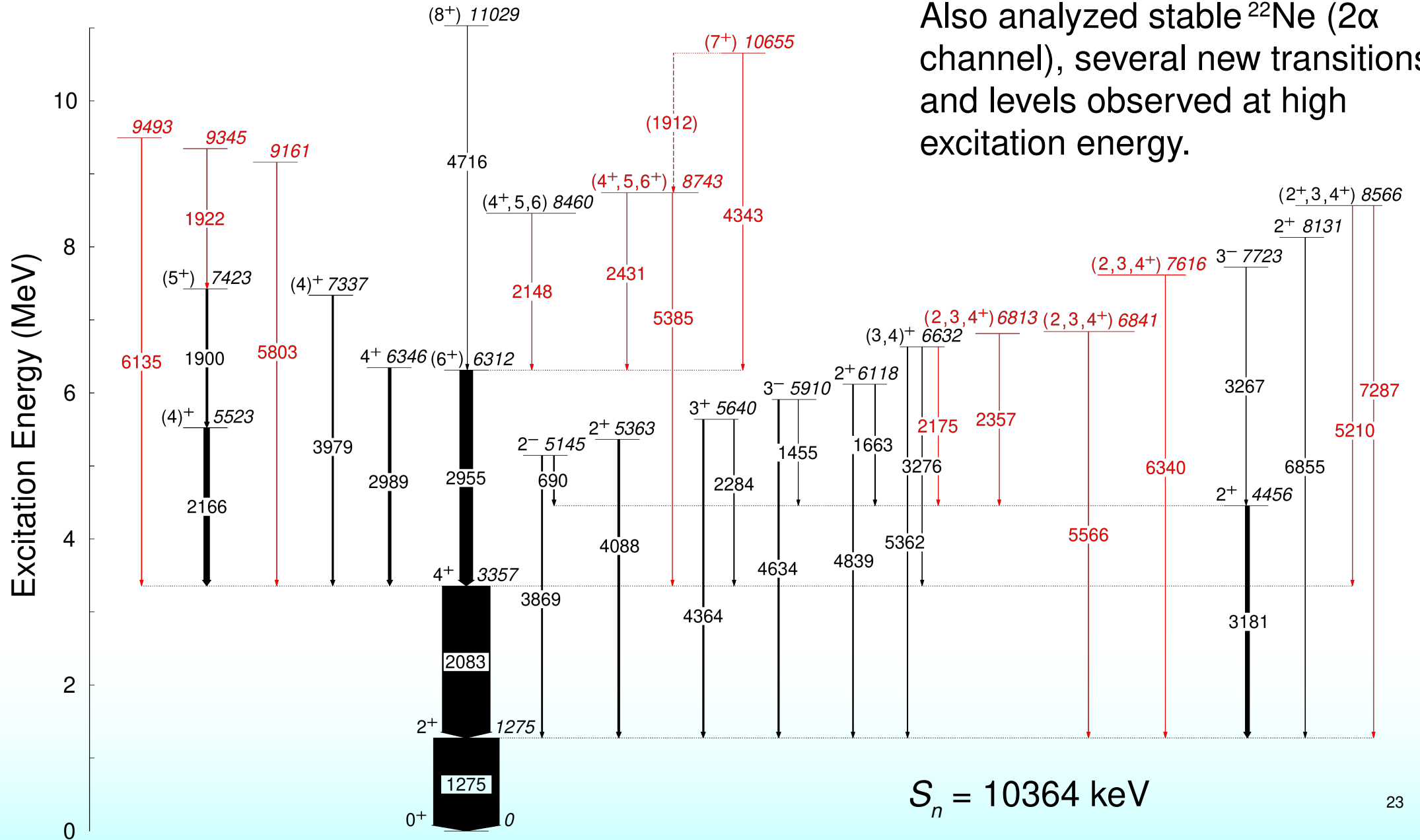
University of Guelph - C. E. Svensson

Louisiana State University – K. D. Launey, G. H. Sargsyan

IIT Roorkee – A. Kumar, P. C. Srivastava, P. Choudhary

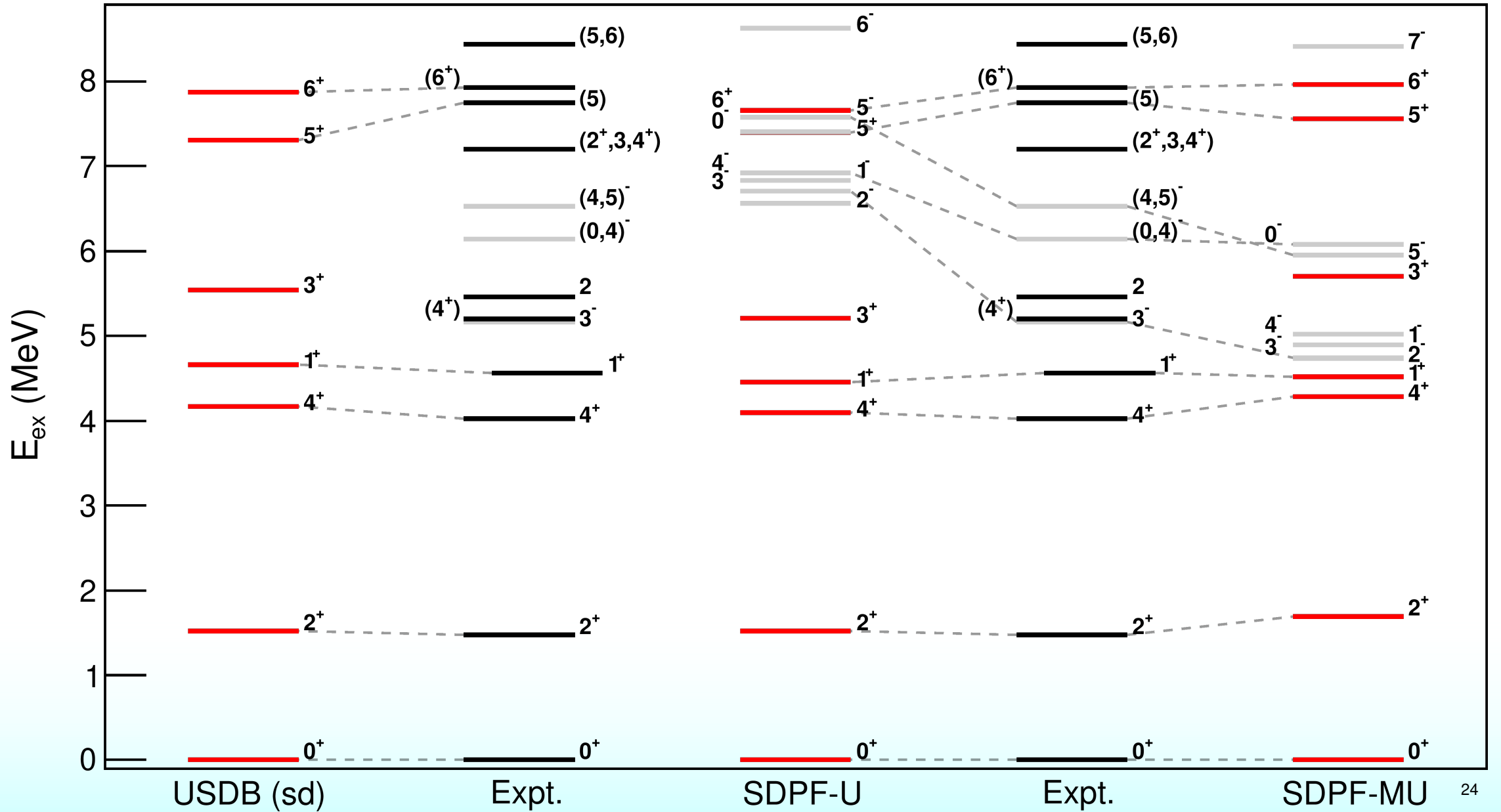


Backup – ^{22}Ne level scheme

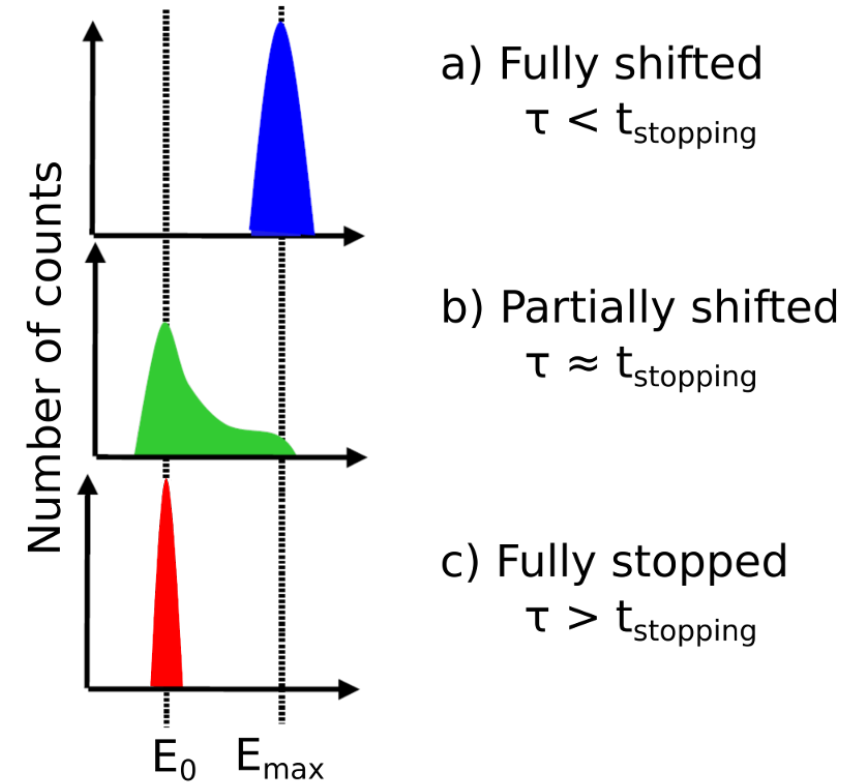
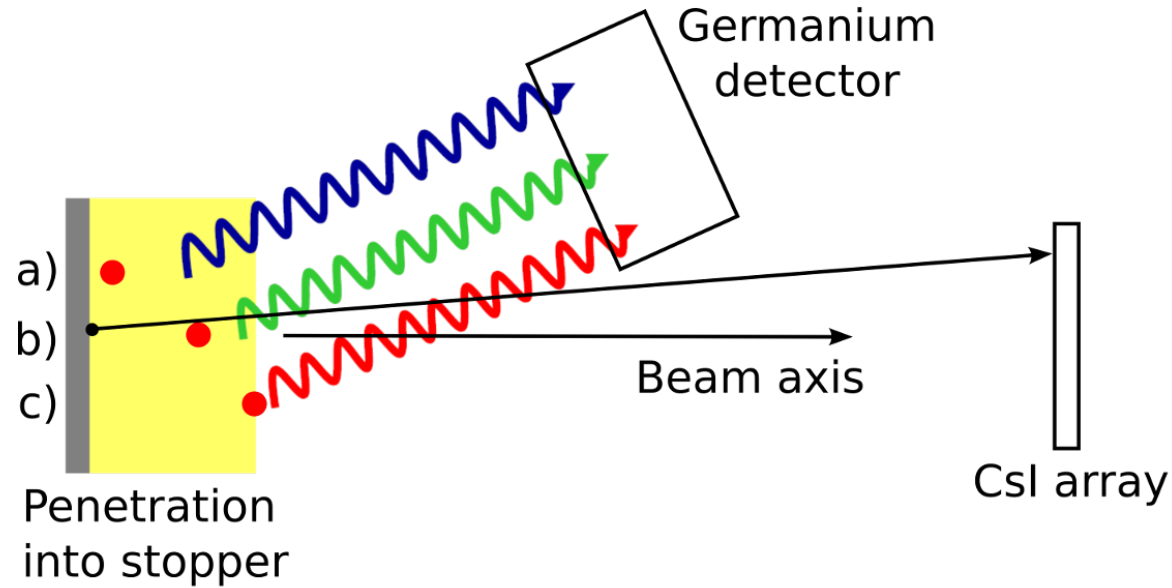


Also analyzed stable ^{22}Ne (2α channel), several new transitions and levels observed at high excitation energy.

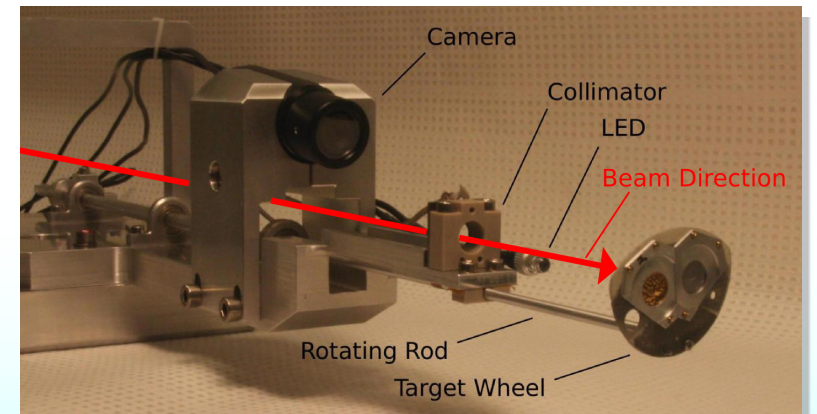
Backup - ^{28}Mg shell model calculations



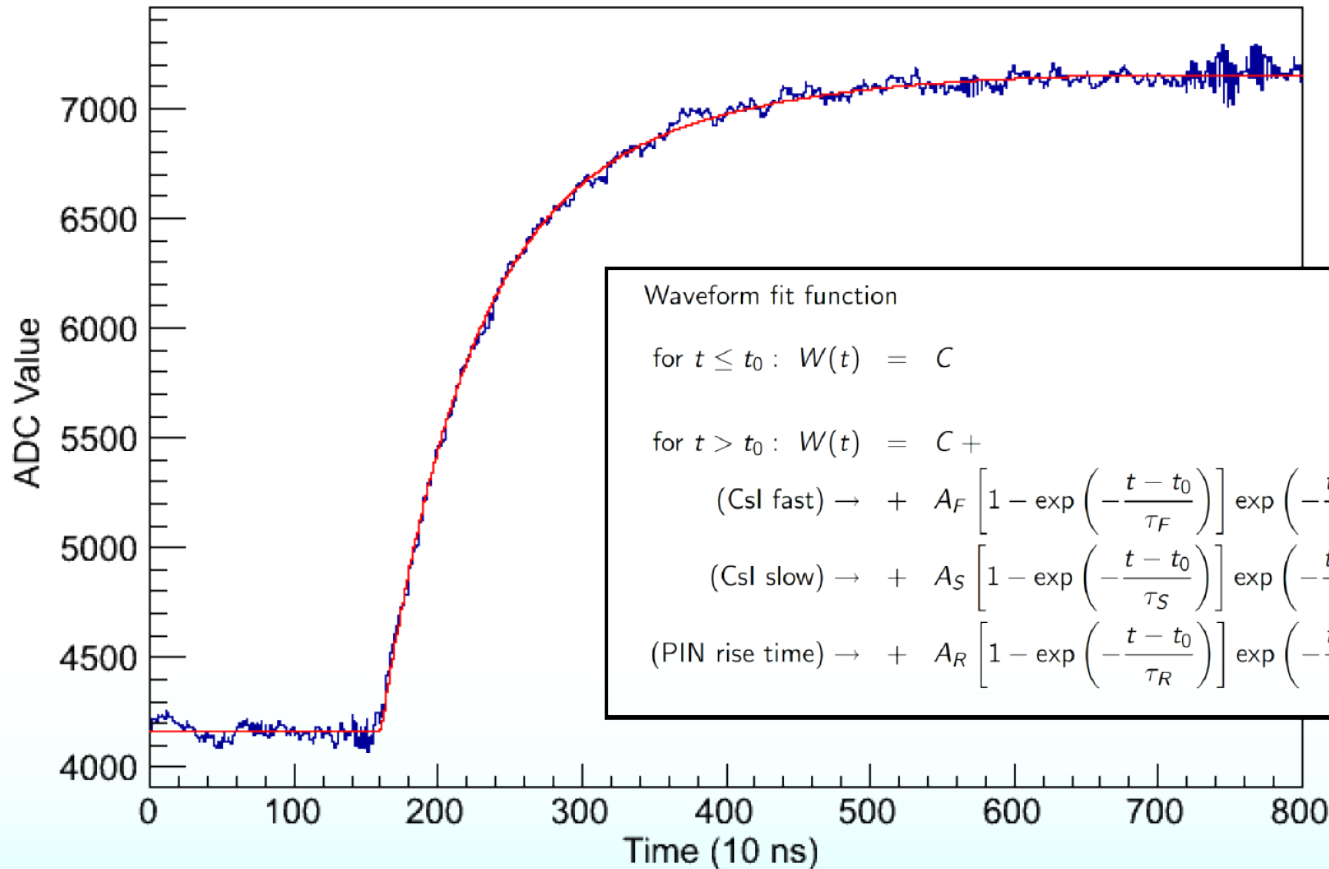
Backup - DSAM Primer



- The species of interest is produced in the target and recoils into a backing, which slows it over time.
- The distribution of Doppler shifted gamma-ray energies observed depends on the mean lifetime of the transition.



Backup – CsI Particle Identification



Waveform fit function

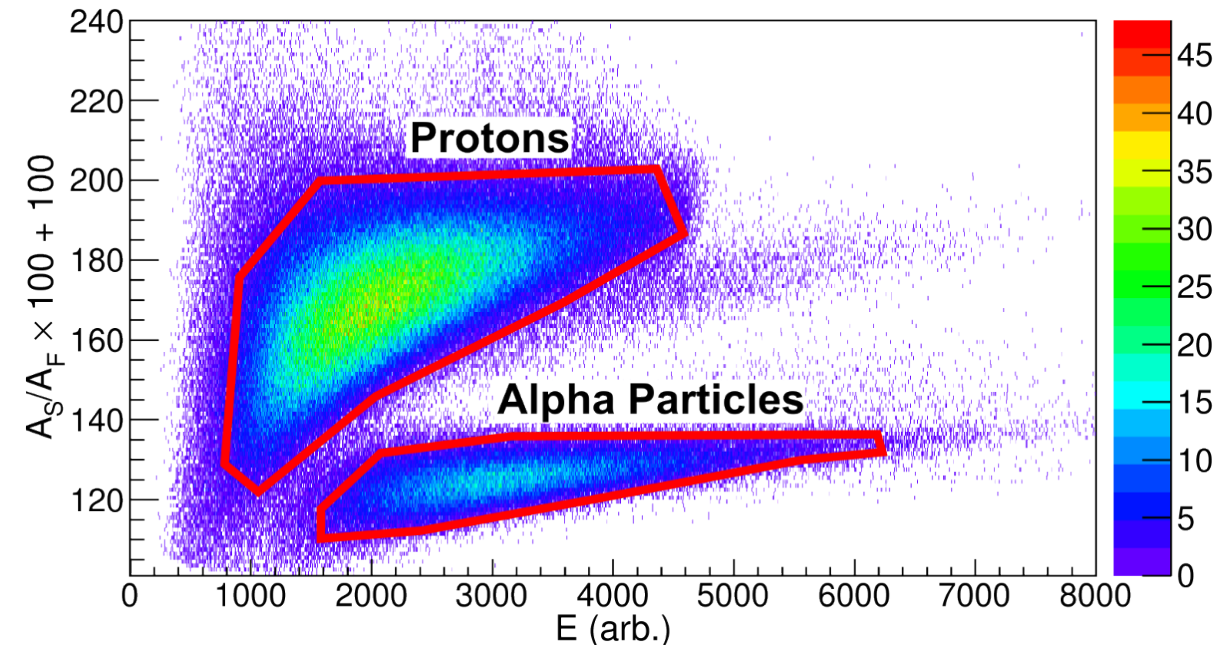
$$\text{for } t \leq t_0: W(t) = C$$

$$\text{for } t > t_0: W(t) = C +$$

$$\text{(CsI fast)} \rightarrow + A_F \left[1 - \exp\left(-\frac{t-t_0}{\tau_F}\right) \right] \exp\left(-\frac{t-t_0}{\tau_{RC}}\right) +$$

$$\text{(CsI slow)} \rightarrow + A_S \left[1 - \exp\left(-\frac{t-t_0}{\tau_S}\right) \right] \exp\left(-\frac{t-t_0}{\tau_{RC}}\right) +$$

$$\text{(PIN rise time)} \rightarrow + A_R \left[1 - \exp\left(-\frac{t-t_0}{\tau_R}\right) \right] \exp\left(-\frac{t-t_0}{\tau_{RC}}\right)$$

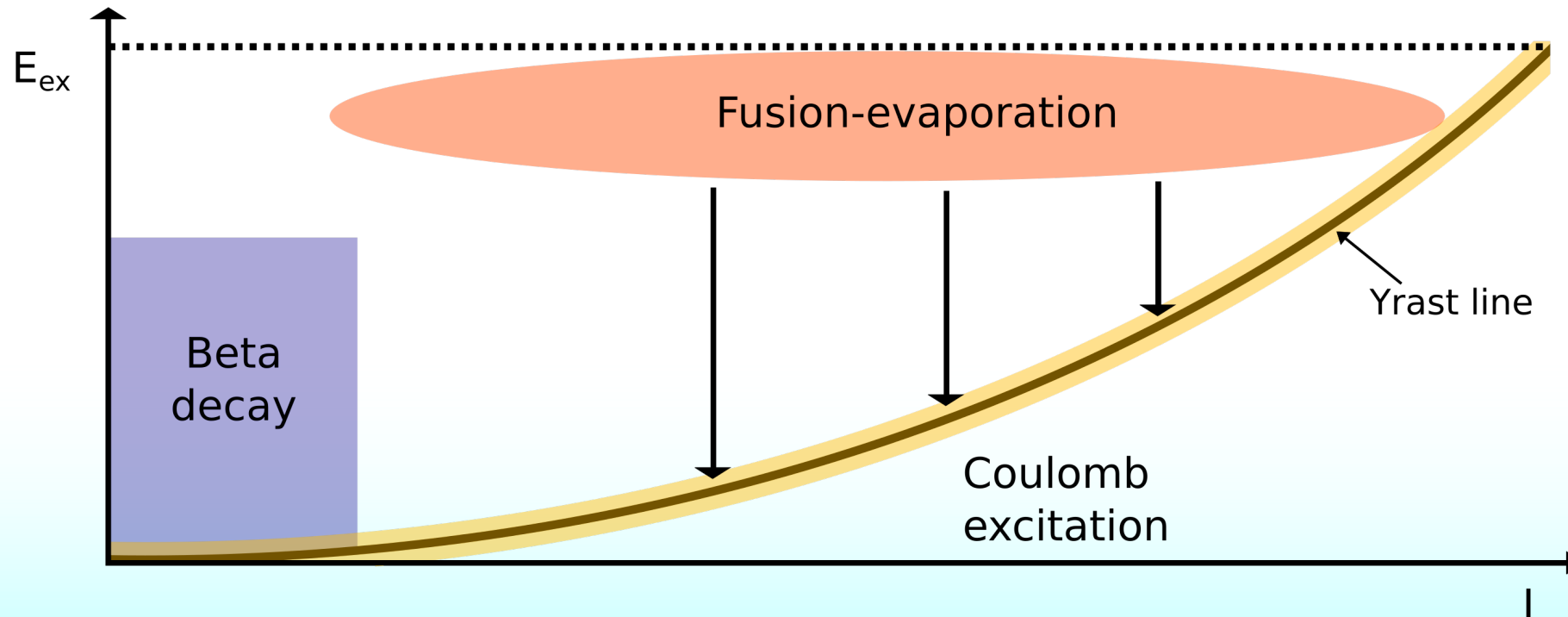


- Particle ID from waveform fit parameters (amplitude ratio of fast and slow components).

Backup – Reaction mechanisms

Fusion-evaporation reactions give access to states in the regime where cross-shell excitations play a role.

- Complementary to existing beta decay studies in the region.
- Multiple channels can be analyzed from a single dataset.
- Identification of charged particles and/or the residual nucleus is needed to separate reaction channels.



Backup – ^{22}Ne data table

E_{level} (keV)	E_{γ} (keV)	This work				Ref. [29]	
		$I_{\gamma,\text{rel}}$	a_2	I^{π}	τ_{mean} (fs)	I^{π}	τ_{mean} (fs)
1274.59(3)	1274.55(3)	1.000(15)	0.25(3)	(2 ⁺)	>3500 ^b	2 ⁺	5190(70)
3357.2(4)	2082.5(4)	0.747(13)	0.30(2)	(4 ⁺)	290(50) ^a	4 ⁺	325(6)
4455.7(10)	3180.9(10)	0.066(3)	0.16(8)	–	<14 ^b	2 ⁺	5(4)
5145.3(10)	690.4(3)	0.0161(15)	–0.31(17)	–	1170(140)	2 [–]	1200(300)
	3869.1(14)	0.0162(16)	–0.78(16)	–			
5363.4(18)	4088.4(18)	0.032(2)	0.02(9)	–	<4 ^b	2 ⁺	100(17)
5523.0(6)	2165.7(5)	0.084(2)	0.56(3)	–	20(5) ^a	(4) ⁺	30(4)
5639.9(13)	2283.5(16)	0.013(2)	–0.1(4)	–	20(8)	3 ⁺	<4
	4364(2)	0.023(2)	–0.09(10)	–			
5910.3(10)	1454.9(7)	0.0040(8)	–0.1(3)	–	71(16)	3 [–]	46(16)
	4634.4(19)	0.024(2)	–0.50(9)	–			
6117.8(15)	1662.6(9)	0.0091(19)	–0.7(4)	–	24(16)	2 ⁺	20(10)
	4839(3)	0.0111(13)	–0.09(15)	–			
6312.0(10)	2954.6(9)	0.206(5)	0.24(3)	(6 ⁺)	57(6)	(6 ⁺)	71(6)
6345.9(13)	2988.5(12)	0.044(2)	0.21(13)	–	16(5)	4 ⁺	19(4)
6632.4(19)	2175(2)	0.0028(7)	–0.3(7)	–	<240 ^a	(3, 4) ⁺	70(30)
	3276(3)	0.0055(10)	–0.3(4)	–			
	5362(5)	0.0083(14)	–0.31(17)	–			
6812.8(17)	2356.9(13)	0.0019(6)	–0.3(6)	(2, 3, 4 ⁺)	160 ⁺¹³⁰ _{–90}	–	–
6841(7)	5566(7)	0.0050(12)	–0.2(2)	(2, 3, 4 ⁺)	<380 ^b	–	–
7337(2)	3979(2)	0.025(2)	0.17(10)	–	<26 ^b	(4) ⁺	50(30)
7423.0(9)	1899.9(6)	0.033(2)	–0.47(19)	–	<40 ^b	(5 ⁺)	<4
7616(7)	6340(7)	0.0052(10)	–0.4(2)	(2, 3, 4 ⁺)	<32 ^b	–	–
7723(2)	3266.9(18)	0.0056(11)	–0.5(6)	–	<22 ^b	3 [–]	–
8131(7)	6855(7)	0.0071(11)	–0.6(2)	–	<31 ^b	2 ⁺	–
8460(3)	2148(3)	0.0056(12)	–0.7(16)	(4 ⁺ , 5, 6)	<110 ^b	–	–
8566(5)	5210(6)	0.0038(8)	0.0(4)	(2 ⁺ , 3, 4 ⁺)	<360 ^b	–	–
	7287(9)	0.0020(7)	0.7(5)	–			
8743(4)	2431(4)	0.0040(10)	–0.1(3)	(4 ⁺ , 5, 6 ⁺)	<40 ^b	–	–
	5385(7)	0.0030(7)	–0.5(5)	–			
9161(5)	5803(4)	0.0069(12)	–0.02(18)	–	70(30)	–	–
9344.6(18)	1921.5(15)	0.0084(17)	0.0(4)	–	<90 ^b	–	–
9493(7)	6135(7)	0.0050(10)	0.0(3)	–	<270 ^b	–	–
10655(5)	1912(7)	<0.0037	–	(7 ⁺)	<120 ^b	–	–
	4343(5)	0.0022(7)	0.9(5)	–			
11029(4)	4716(3)	0.0017(9)	0.5(6)	(8 ⁺)	<64 ^b	(6 ⁺ , 8 ⁺)	–

^aCorrected for feeding from an observed transition.

^bLimit reported to a 90% confidence level.

Backup – ^{25}Na data table

This work						Previous results (see footnotes)	
E_{level} (keV)	E_{γ} (keV)	$I_{\gamma,\text{rel}}$	a_2	I^{π}	τ_{mean} (fs)	I^{π}	τ_{mean} (fs)
92(3)	–	–	–	–	–	$3/2^{+f}$	$7.4(4) \times 10^{6f}$
1072(4)	980.4(5)	0.170(14)	−0.7(3)	–	>800 ^b	$1/2^{+f}$	1900(200) ^f
2204(4)	1131.8(4)	0.069(12)	−0.1(3)	–	26(11)	$3/2^{+f}$	36(6) ^f
2419.8(11)	2419.6(11)	1.00(3)	0.30(3)	(9/2 ⁺)	230(40) ^a	$9/2^{+c}$	240(40) ^c
2791.0(12)	2699(3)	0.018(4)	0.9(3)	–	150(20) ^a	$7/2^{+c}$	190(35) ^c / 250(50) ^d
	2790.8(13)	0.192(15)	0.39(14)	–	–	–	–
3355(3)	3355(3)	0.045(16)	−0.2(3)	–	<49 ^b	(7/2) ^{+c}	23(7) ^f
3460.9(9)	669.1(7)	0.022(3)	−0.4(2)	(9/2 ⁺)	190(30) ^a	$9/2^{+c}$	210(25) ^f / 130(40) ^c
	1041.3(4)	0.427(11)	0.12(3)	–	–	–	–
	3462(3)	0.032(11)	−0.1(7)	–	–	–	–
3963(4)	2891(3)	0.026(9)	0.0(5)	(1/2, 3/2, 5/2 ⁺)	<250 ^b	(1/2 ⁺ , 3/2, 5/2 ⁺) ^f	< 140 ^f
3999.6(11)	1209.0(4)	0.135(10)	−0.31(9)	–	90(7)	$9/2^{+c}$	100(20) ^c
	1579.1(13)	0.028(4)	0.0(3)	–	–	–	–
4005(5)	2933(3)	0.026(9)	−0.8(6)	(1/2, 3/2)	90(50)	–	45(10) ^f
4294(5)	3222(3)	0.030(10)	−0.4(7)	–	<29 ^b	$1/2^{+f}$	–
4967.3(8)	967.3(9)	0.011(3)	−0.2(5)	–	72(6) ^a	(11/2) ^{+c}	–
	1506.2(6)	0.244(10)	−0.70(8)	–	–	–	80(20) ^c
	2548.0(12)	0.140(9)	−0.03(13)	–	–	–	120(30) ^c
5231(2)	1875.0(12)	0.04(2)	0.3(2)	(7/2, 9/2)	<15 ^b	–	–
	2441(3)	0.009(3)	−0.9(9)	–	–	–	–
5388.4(18)	2968.4(15)	0.170(10)	−0.15(13)	(11/2 ⁺)	<4 ^b	(9/2, 11/2) ^{+c}	–
5749(4)	3329(4)	0.016(3)	0.1(4)	(9/2, 11/2, 13/2)	<280 ^b	–	–
5848(3)	3058(3)	0.014(3)	0.9(5)	–	<75 ^b	$7/2^{+c}$	–
	3427(4)	0.017(3)	0.1(4)	–	–	–	–
6271(5)	3480(4)	0.010(2)	−0.3(7)	(9/2, 11/2)	<37 ^b	–	–
	3851(5)	<0.004	–	–	–	–	–
6381(3)	2924(5)	0.018(5)	−0.6(8)	(9/2, 11/2, 13/2)	<9 ^b	–	–
	3958(4)	0.037(4)	−0.1(2)	–	–	–	–
6581(2)	3120(4)	0.020(4)	−0.2(7)	–	<40 ^b	(11/2) ^{-c}	–
	4163(4)	0.027(3)	−0.1(3)	–	–	–	–
6736.6(19)	1348.9(13)	0.021(5)	0.3(3)	(13/2 ⁺)	<4 ^b	–	–
	1770.7(16)	0.064(8)	−0.3(2)	–	–	–	–
	3275(6)	0.012(4)	−0.1(10)	–	–	–	–
	4313(3)	0.053(4)	0.3(2)	–	–	–	–
6854(2)	1467.9(10)	0.026(4)	−0.6(3)	(13/2 ⁺)	60(40)	(11/2, 13/2) ^{+c}	–
	3395(5)	0.015(4)	−0.7(7)	–	–	–	–
	4436(3)	0.031(3)	0.5(4)	–	–	–	–
7218(4)	3218(4)	0.012(3)	0.6(4)	(9/2, 11/2, 13/2)	<140 ^b	–	–
	4796(9)	0.006(2)	−1.4(13)	–	–	–	–
7626(4)	2658(4)	0.027(5)	−0.6(4)	(11/2, 13/2)	<75 ^b	–	–

^aCorrected for feeding from an observed transition.

^bLimit reported to a 90% confidence level.

^cPrevious result from Ref. [8].

^d[26].

^e[27].

^f[28].

Backup – ^{28}Mg data table

Level energy (keV)	Gamma rays (keV)	This work			Ref. [19]	
		$I_{\gamma,\text{rel}}$	I^π	τ_{mean} (fs)	I_{eval}^π	$\tau_{\text{mean,eval}}$ (fs)
1473.63(9)	1473.59(9)	1.000(15)		$>1.5 \times 10^3$ ^a	2 ⁺	$1.73(14) \times 10^3$
4021.4(3)	2547.6(3)	0.65(2)	4 ⁺	$1.8(3) \times 10^2$	4 ⁺	$1.5(5) \times 10^2$
4556.3(12)	3082.5(12)	0.119(16)		<42 ^a	2 ⁺	<43
4879(2)	3405(2)	0.023(7)		<26 ^a	2 ⁺	$<1.2 \times 10^2$
5172.9(7)	3698(3), 1151.5(6)	0.08(2), 0.031(10)		$2.6_{-1.3}^{+1.6} \times 10^2$	3 ⁻	$1.6(13) \times 10^2$
5184.3(5)	1163.1(4)	0.120(9)	(4 ⁺)	21_{-14}^{+15}		
5475(3)	4001(3)	0.018(8)		$<5.0 \times 10^2$ ^a	2	
5672(3)	4198(3)	0.048(10)		$1.1(4) \times 10^2$	2 ⁺	
6139.0(12)	4664.9(12)	0.032(9)	(0, 4) ⁻	$>1.0 \times 10^3$ ^a , $<2.5 \times 10^5$ ^b		
6528.2(9)	1356.3(12), 2506.7(8)	0.021(5), 0.115(12)	(4, 5) ⁻	$1.9(6) \times 10^2$		
7203(3)	3181(3), 5723(5)	0.033(10), 0.009(4)	(2 ⁺ , 3, 4 ⁺)	$<3.8 \times 10^2$ ^a		
7747(2)	3726(2)	0.033(8)	(5)	<85 ^a		
7929.3(12)	3907.6(12)	0.060(11)	(6 ⁺)	<42 ^a		
8438(5)	4416(5)	0.024(10)	(5,6)	$<1.5 \times 10^3$ ^b	(6 ⁺)	

^aLimit reported to a 90% confidence level.

^bLimit estimated based on lineshape (see text).